

# Cellular and Molecular Life Sciences

## Autoinhibition of TBCB regulates EB1-mediated microtubule dynamics

--Manuscript Draft--

<b>Manuscript Number:</b>	
<b>Full Title:</b>	Autoinhibition of TBCB regulates EB1-mediated microtubule dynamics
<b>Article Type:</b>	Research article
<b>Corresponding Author:</b>	Juan Carlos Zabala, PhD Universidad de Cantabria Santander, Cantabria SPAIN
<b>Corresponding Author Secondary Information:</b>	
<b>Corresponding Author's Institution:</b>	Universidad de Cantabria
<b>Corresponding Author's Secondary Institution:</b>	
<b>First Author:</b>	Gerardo Carranza, PhD
<b>First Author Secondary Information:</b>	
<b>Order of Authors:</b>	Gerardo Carranza, PhD Raquel Castaño, PhD Monica L Fanarraga, PhD Juan Carlos Villegas, PhD Joao Gonçalves, PhD Helena Soares, PhD Jesus Avila, PhD Marco Marenchino, PhD Ramón Campos-Olivas, PhD Guillermo Montoya, PhD Juan Carlos Zabala, PhD
<b>Order of Authors Secondary Information:</b>	
<b>Abstract:</b>	<p>Tubulin cofactors (TBCs) participate in the folding, dimerization, and dissociation pathways of the tubulin dimer. Among them, TBCB and TBCE are two CAP-Gly domain-containing proteins that interact and dissociate the tubulin dimer. Here we show how TBCB localizes at spindle and midzone microtubules during mitosis. Furthermore, the motif DEI/M-COO- present in TBCB, which is similar to the EEY/F-COO- element characteristic of EB proteins, CLIP-170, and <math>\alpha</math>-tubulin, is required for TBCE-TBCB heterodimer formation and thus for tubulin dimer dissociation. This motif is responsible for TBCB autoinhibition, and our analysis suggests that TBCB is a monomer in solution. Mutants of TBCB lacking this motif are derepressed and induce microtubule depolymerization through an interaction with EB1 associated to microtubule tips. TBCB is also able to bind to the chaperonin complex CCT containing <math>\alpha</math>-tubulin, suggesting that it could escort tubulin to facilitate its folding and dimerization, recycling or degradation.</p>
<b>Suggested Reviewers:</b>	Jadwiga Chroboczek wisia@ibs.fr Expert, recently has published a review in CMLS  John Correia jcorreia@biochem.umsm.edu biophysicist, Expert in cytoskeleton and microtubules

	Leslie Wilson wilson@lifesci.ucsb.edu Expert in tubulins, end binding proteins and microtubules
	Tim Stearns stearns@stanford.edu expert in centrosome, microtubules and TBCs
<b>Opposed Reviewers:</b>	

## Autoinhibition of TBCB regulates EB1-mediated microtubule dynamics

Gerardo Carranza<sup>\*</sup>, Raquel Castaño<sup>\*</sup>, Mónica L. Fanarraga<sup>\*</sup>, Juan Carlos Villegas<sup>\*</sup>, João Gonçalves<sup>†</sup>, Helena Soares<sup>†</sup>, Jesus Avila<sup>‡</sup>, Marco Marenchino<sup>§</sup>, Ramón Campos-Olivas<sup>§</sup>, Guillermo Montoyal, and Juan Carlos Zabala<sup>\*</sup>

<sup>\*</sup>Departamentos de Biología Molecular y Celular, Facultad de Medicina, IFIMAV-Universidad de Cantabria, 39011 Santander, Spain

<sup>†</sup> Centro de Química e Bioquímica da Faculdade de Ciências da Universidade de Lisboa, 1749-016 Lisboa and Instituto Gulbenkian de Ciência, Ap. 14, 2781-901 Oeiras and Escola Superior de Tecnologia da Saude de Lisboa, 1990-096 Lisboa, Portugal

<sup>‡</sup>Centro de Biología Molecular (CSIC-UAM), Universidad Autónoma de Madrid, 28049 Cantoblanco, Madrid, Spain

<sup>§</sup>Spectroscopy and NMR Unit and <sup>l</sup>Macromolecular Crystallography Group, Structural Biology and Biocomputing Program, Spanish National Cancer Research Center (CNIO), Melchor Fdez. Almagro 3, 28029 Madrid, Spain

Contact information:

Juan Carlos Zabala

Phone 34 942201949

Email: zabalajc@unican.es

Present address for João Gonçalves:

Samuel Lunenfeld Research Institute

Mount Sinai Hospital

600 University Avenue, Room 1070

Toronto Ontario M5G 1X5

Canada

Footnotes: CCT/Microtubule Dynamics/+TIPs/Tubulin Folding Cofactors

Running title: TBCB autoinhibition and EB1 binding at MT ends

## Abstract

Tubulin cofactors (TBCs) participate in the folding, dimerization, and dissociation pathways of the tubulin dimer. Among them, TBCB and TBCE are two CAP-Gly domain-containing proteins that interact and dissociate the tubulin dimer. Here we show how TBCB localizes at spindle and midzone microtubules during mitosis. Furthermore, the motif DEI/M-COO<sup>-</sup> present in TBCB, which is similar to the EEY/F-COO<sup>-</sup> element characteristic of EB proteins, CLIP-170, and  $\alpha$ -tubulin, is required for TBCE-TBCB heterodimer formation and thus for tubulin dimer dissociation. This motif is responsible for TBCB autoinhibition, and our analysis suggests that TBCB is a monomer in solution. Mutants of TBCB lacking this motif are derepressed and induce microtubule depolymerization through an interaction with EB1 associated to microtubule tips. TBCB is also able to bind to the chaperonin complex CCT containing  $\alpha$ -tubulin, suggesting that it could escort tubulin to facilitate its folding and dimerization, recycling or degradation.

## Introduction

The cytoskeleton of eukaryotic cells is required for many essential cell processes such as motility, organelle and membrane structural integrity, intracellular trafficking, chromosome segregation, and cytokinesis [1]. Microtubules are complex polar polymers of the cytoskeleton that assemble from  $\alpha\beta$ -tubulin heterodimers. The heterodimers polymerize, forming protofilaments that associate laterally, forming the wall of a hollow cylinder, the microtubule [2,3]. Therefore, within the microtubule lattice, each single  $\alpha$ -tubulin or  $\beta$ -tubulin subunit interacts with four other neighboring tubulin subunits. In fact, each  $\alpha$ -tubulin subunit interacts with its  $\beta$ -tubulin partner inside of the heterodimer, with a second  $\beta$ -tubulin subunit from the preceding heterodimer in the protofilament, and laterally with two  $\alpha$ -subunits from the two side protofilaments. Thus, the assembly of a microtubule, while preventing unwanted interactions, is a highly complex task that must be properly controlled to avoid critical errors.

Tubulin folding cofactors (TBCs) are a set of different proteins discovered a decade ago in the so-called "postchaperonin" tubulin folding pathway. TBCs are responsible for the achievement of the quaternary conformation of the  $\alpha\beta$ -heterodimer after tubulin monomers have reached their tertiary structure [4,5]. More recent studies have shown that *in vivo*, these proteins are implicated in microtubule dynamics through their ability to dissociate the tubulin heterodimer, and probably by controlling tubulin monomer quality and exchange (shuffling mechanism) [6-8].

TBCB and TBCE are two well-conserved  $\alpha$ -tubulin interacting proteins that collaborate in the regulation of microtubule dynamics [6-9]. Both cofactors participate in the  $\alpha$ -tubulin folding pathway and are required for cell survival [5, 10], playing important roles *in vivo* as revealed by the plethora of human disorders in which they are implicated. TBCE mutations cause a syndrome called hypoparathyroidism-retardation-dysmorphism, also known as the Sanjad-Sakati syndrome [11] in humans, and a progressive motor neuropathy in the mouse [12]. TBCB, on the other hand, has been implicated in human

1  
2  
3  
4 cancer [13], neurodevelopmental malformations [14], schizophrenia [15], and  
5 neurodegenerative processes [16].

6 TBCB shares with TBCE two similar domains, a CAP-Gly domain at the N-terminus,  
7 and a UBL domain at the C-terminus, but while TBCB it is not able to interact with or  
8 dissociate the tubulin heterodimer by itself, TBCE is, per se, effective in promoting this  
9 dissociation. Nonetheless, TBCE interacts with TBCB, originating the TBCE–TBCB  
10 complex, which displays a more efficient stoichiometric tubulin dissociation activity than  
11 TBCE alone. Upon dissociation, TBCB, TBCE, and  $\alpha$ -tubulin form a stable ternary  
12 complex. The disassembly of this ternary complex results in either TBCB and  $\alpha$ -tubulin,  
13 and free TBCE, or TBCE and  $\alpha$ -tubulin, and free TBCB. Free  $\beta$ -tubulin subunits might  
14 be recyclable in the presence of TBCE or TBCD [9].

15 The function of the CAP-Gly domains of both cofactors is still unknown. This domain is  
16 a protein-interaction module that typically plays a role controlling microtubule end  
17 dynamics in end-binding proteins (EBs), which can track along microtubule ends [17-19].  
18 In addition to EBs, an increasing number of proteins that control microtubule  
19 organization and dynamics, known as microtubule plus-end-tracking proteins (+TIPs),  
20 have been identified. These proteins connect to the microtubule plus ends through an  
21 interaction with members of the EB family [17-19], the only known protein family that  
22 can track microtubule ends autonomously. Recently, a long list of +TIPs candidates has  
23 been published by Yu et al. (2011) [20], but neither TBCB nor TBCE has been included.  
24 In this work, we have used a multidisciplinary approach to study the molecular  
25 mechanism of TBCB's regulation of microtubule dynamics. For this purpose, we have  
26 cloned the human *Tbcb* gene and characterized mutant versions of its product, having  
27 established that the last three amino-acid residues of this protein are crucial for TBCB  
28 autoinhibition. In fact, the overexpression of the mutated form of TBCB lacking the  
29 DEI/M-COO<sup>-</sup> motif, similar to the EEY/F-COO<sup>-</sup> element in EB1 and related proteins,  
30 produces a massive microtubule destruction in vivo. Using extensive biophysical and  
31 biochemical approaches, we unmasked the molecular mechanism by which TBCB  
32 controls microtubule depolymerization by means of EB1. In addition, we show for the  
33 first time that TBCB interacts directly with cytosolic chaperonin containing TCP-1  
34 (CCT) during the folding process of  $\alpha$ -tubulin. All the results obtained from this work led  
35 us to propose three different models to explain the autoinhibition of TBCB, its role in  
36 tubulin folding as a CCT cofactor, and the mechanism by which the deregulation of  
37 TBCB activity induces the microtubule catastrophe in living cells.  
38  
39  
40  
41  
42  
43  
44  
45  
46  
47  
48  
49

## 50 **Materials and Methods**

### 51 **Human TBCB gene cloning**

52 The human *tbcb* coding sequence was amplified by PCR from a testis cDNA sample (BD  
53 Biosciences, USA) using a pair of primers designed with the appropriate restriction  
54 enzyme recognition sites at their ends: forward primer 5' GTG AAG CTT CAT ATG  
55 GAG GTG ACG GGG GTG 3'; reverse primer 5' CGC GGA TCC TCA TAT CTC GTC  
56  
57  
58  
59  
60  
61  
62  
63  
64  
65

1  
2  
3  
4 CAA CCC 3'. The amplified coding sequence was then inserted in the *HindIII* and  
5 *BamHI* sites of the mammalian expression vector pcDNA3.1 (Invitrogen, Life  
6 Technologies, USA) to generate the pcDNA3.1-TBCB recombinant plasmid. Human  
7 TBCB was cloned into the pEYFP vector from Clontech (Clontech Laboratories, USA).  
8 TBCB $\Delta$ 3 and TBCB $\Delta$ 9 cDNA fragments were produced by PCR. The resulting  
9 fragments were cloned into pET29c and sequenced (EMD Millipore Bioscience  
10 Novagen, USA).  
11  
12

### 13 14 **TBCA and TBCE protein purification and characterization**

15  
16 Human TBCE cDNA wild-type (accession number U61232) and human TBCA [21] were  
17 His-tagged at the C-terminus and cloned into the pRJ-pFastBac vector [8] for  
18 recombinant baculovirus production using the Bac-to-Bac Baculovirus Expression  
19 System (Invitrogen, Life Technologies, USA). These were then used to infect  
20 commercially obtained Sf9 insect cells to produce recombinant TBCE, which was  
21 purified following protocols already described elsewhere with minor modifications [8,9].  
22 TBCA<sup>His</sup> was purified from a 50 mL culture of Sf9 cells infected with baculoviruses  
23 carrying the human TBCA<sup>His</sup> cDNA cloned. Cells were pelleted by centrifugation,  
24 washed, and stored frozen at  $-70^{\circ}\text{C}$ . Pellets were resuspended in 7.5 mL of 0.5 mM Tris  
25 buffer (pH 8) containing protease inhibitors and sonicated three times during 20 seconds  
26 at  $4^{\circ}\text{C}$ . Extract was spun at  $60,000 \times g$  in a Ti 50.2 ultracentrifuge rotor (Beckman-  
27 Coulter) for 30 min at  $4^{\circ}\text{C}$ . Supernatant was supplemented with a buffer stock to produce  
28 final concentrations of 50 mM Tris-buffer (pH 8) and 500 mM NaCl and 10 mM  
29 imidazole and loaded into a 1 mL His-Trap column (GE Healthcare). Fractions  
30 containing TBCA–His were pooled and concentrated by ultrafiltration using an Amicon  
31 Ultra 10K filter (Millipore, USA). Protein concentrate was applied to a high-resolution  
32 gel-filtration column (Superdex-75 HR, GE Healthcare, USA), equilibrated and eluted  
33 with 20 mM Bis-Tris buffer (pH 7) containing 100 mM KCl, 1 mM DTT and 0.5 mM  
34 PMSF at 0.4 mL/min.  
35  
36  
37  
38  
39

### 40 41 **Nonclassical two-dimensional electrophoresis**

42  
43 In the first dimension, the protein complexes were fractionated by charge and shape, and  
44 then were denatured and their molecular composition determined in the second  
45 dimension. The samples were loaded onto a native 0.75 mm thick minigel (7 cm  $\times$  8 cm)  
46 as described [22, 23]. After two hours of electrophoresis, a single running lane containing  
47 the native electrophoresed sample was excised with a blade on glass, loaded onto a  
48 preparative 1.5 mm thick SDS-minigel (7 cm  $\times$  8 cm), and fixed to the gel with 0.5%  
49 agarose prepared in 1 $\times$  SDS loading buffer. Denaturing electrophoresis was performed  
50 for three hours at 10 mA constant current, after which the gel was stained with  
51 Coomassie Blue G-250. In a similar manner, bands of interest were excised with a blade  
52 on glass, dried in a Speed-Vac concentrator (Thermo Fisher Scientific, USA) and  
53 rehydrated with loading 1 $\times$  SDS loading buffer, heated at  $90^{\circ}\text{C}$  for 2 min, and loaded  
54 onto a regular 8.5% SDS minigel. Electrophoresis was performed as described above.  
55  
56  
57  
58  
59  
60  
61  
62  
63  
64  
65

## **Antisera production, immunocytochemistry, and cell cultures**

Affinity-purified primary antibodies were produced against purified human TBCB recombinant protein. Rabbit sera were affinity purified as described previously [24]. For immunocytochemistry, the antibodies used were anti- $\alpha$ - and anti- $\beta$ -tubulin (B512 and Tub2.1, respectively) and anti-acetylated tubulin from Sigma-Aldrich. The anti-glutamylated tubulin antibody (GT335) was a gift from Dr. Janke (CNRS, Montpellier, France). Secondary antibodies were Alexa-Fluor-488-conjugated goat anti-rabbit IgG and goat-anti-mouse IgG, Alexa-Fluor-647-conjugated goat anti-mouse IgG (Molecular Probes, Invitrogen), Cy3-conjugated goat anti-mouse IgG and goat anti-mouse IgG<sub>1</sub>, and Cy5-conjugated goat anti-rabbit IgG (Jackson ImmunoResearch Laboratories). For some experiments, microtubules were depolymerized with 2  $\mu$ M nocodazole and cold (4°C) treatments for 30 min.

## **Microtubule depolymerization experiments**

Bovine brain tubulin was purified as described [25]. Purified tubulin was incubated at 35°C for 20 minutes, and as a control, TBCB or ovalbumin was added for another 20 minutes in buffer A (MES 100 mM pH 6.7, EGTA 1 mM, and MgCl<sub>2</sub> 1 mM) with 2 mM GTP and 30% glycerol. The pellet and supernatant were separated after centrifugation at 45,000  $\times$ g for 1 hour at 30°C through a 50% sucrose cushion containing 1 mM GTP.

## **Fractionation by gel filtration of complexes formed between cofactors TBCB and TBCE and TBCB**

Purified tubulin cofactors and complexes formed in reactions conducted at 30°C for 30 minutes were fractionated in a Superdex 200 PC 3.2/30 gel-filtration precision column using an Ettan LC (GE Healthcare) at room temperature. The elution buffer contained 0.1 M MES (pH 6.7), 1 mM MgCl<sub>2</sub>, 1 mM EGTA, and 25 mM KCl. Fractions of 25  $\mu$ L were eluted at 40  $\mu$ L/min and were analyzed by SDS-PAGE.

## **Confocal microscopy, cell counts, and statistical analysis**

Transitory transfection experiments were performed using Lipofectamine Plus reagent (Life Technologies) or the FuGene 6 reagent (Roche) following the manufacturer's instructions. The GFP:EB1 construct was kindly supplied by Dr. Akhmanova (Utrecht University, The Netherlands). Cell counts in Figure 1C were performed at 30 h post transfection using a 63 $\times$  Zeiss oil immersion objective starting from a random field and scanning horizontally from that point. Values presented in the histogram of Figure 1C were obtained by double immunofluorescence with anti- $\alpha$ -tubulin/TBCB. Values in Figure 5D were obtained by double immunofluorescence with anti- $\alpha$ -tubulin/TBCB combined with Hoechst 33258 and GFP labeling in cotransfection experiments. Cell counts were performed on confocal microscopy projection images using a Nikon A1R LSM confocal microscope equipped with an argon (488 nm) laser, two HeNe (564 and 633 nm) lasers, and a diode (405 nm) laser. Only cells with no microtubules, which

1  
2  
3  
4 presented healthy-looking nuclei, as assessed by Hoechst staining, were considered. In  
5 colocalization experiments, images were scanned sequentially to avoid fluorescent  
6 channel emission cross talk / bleed through. A *t* test was performed on data obtained from  
7 two different coverslips of at least three different experiments. Statistical analysis of data  
8 and graphing were performed using SigmaPlot 8.0 software (Systat Software, Richmond,  
9 CA). Histograms represent mean values and standard error bars.

## 12 **Tubulin dimer dissociating assay and nondenaturing electrophoresis**

13  
14 Aliquots of purified brain tubulin were mixed with different amounts of purified TBCE in  
15 15  $\mu$ L reactions containing 50 mM MES (pH 6.7), 1 mM  $MgCl_2$ , and 1 mM GTP in the  
16 absence and presence of a stoichiometric excess of TBCB or TBCB $\Delta$ 3, and incubated for  
17 30 min at 30°C. The reaction mixtures were diluted with a sucrose-containing native  
18 loading buffer and loaded onto a 6% nondenaturing polyacrylamide gel [22, 23]. Native  
19 gels were stained directly with Coomassie Brilliant Blue.

## 23 **Affinity chromatography**

24  
25 Purified TBCB $\Delta$ 3 was coupled specifically at its amino terminus using EDC-NHS  
26 coupling chemistry in a Hi-trap NHS-activated HP column (GE Healthcare). This column  
27 gave us complete control over the experimental conditions (extract preparation, column  
28 loading, bound partner elution, time, and temperature). Thus, HEK293 cell extracts were  
29 prepared, sonicated to fragment microtubules, and loaded into the column at 4°C, to  
30 avoid protein degradation. We used a slow loading rate, to allow binding of the  
31 interactors to the column. 300 mg of HEK293 were resuspended and subject to a  
32 hypotonic shock in Tris buffer 20 mM (pH 7.3) and PMSF 0.5 mM (buffer H).  
33 Subsequently, cells were sonicated three times during 30 s at 130 watts at 4°C. Protein  
34 extract (1 mL at 18 mg/mL) obtained from human HEK293 cells was applied to the NHS  
35 column equilibrated in buffer H. The column was washed with 10 mL of the same buffer,  
36 and specifically interacting proteins (detail) were eluted with a NaCl gradient (red line).

## 41 **Results**

### 44 **Auto-inhibition of TBCB**

45  
46 TBCB is encoded by a unique gene in the human genome. This protein is composed of  
47 two functional structural domains connected by a coiled-coil segment (Fig 1A). At the N-  
48 terminus, TBCB contains a ubiquitin-like domain. This domain is spherical (PDB ID,  
49 1V6E), behaves as a monomer of about 14 kDa and is a ubiquitous protein interaction  
50 domain present in many unrelated proteins. The C-terminal domain is a CAP-Gly  
51 characteristic of +TIPs proteins. This domain is also globular, with a three-layer  $\beta$ - $\beta$   
52 structure (three antiparallel  $\beta$ -sheets), as represented by the *C. elegans* F53f4.3 protein  
53 CAP-Gly domain (Fig 1A, PDB: 1TOV, [26]). The unique  $\alpha$ -helix is preceded by a  
54 disordered stretch of 17 residues, and the last 6–7 amino acid residues protrude from the  
55 globular domain. CAP-Gly domains serve as recognition domains for EEY/F-COO<sup>-</sup>



1  
2  
3  
4 peptides [27]. This sequence assumes an extended conformation, and the side chain of the  
5 terminal tyrosine packs with several hydrophobic amino acid residues in the CAP-Gly  
6 domain [28]. The crystal structure of the CAP-Gly of TBCB (*C. elegans*) revealed that  
7 this domain consists of 84 amino acid residues, and although it does not form a dimer in  
8 vitro, the conserved groove, involved in the interaction with EEY/F-COO<sup>-</sup> elements  
9 characteristic of EB, CLIP-170, and  $\alpha$ -tubulin, holds the C-terminal peptide of the  
10 neighboring molecule in the asymmetric unit of the crystal [26].

11  
12 The structural prediction [29] for the human TBCB's last nine amino acid residues (Fig  
13 1a) is that of a disordered peptide, protruding from the globular domain and thus being  
14 able to interact with a CAP-Gly domain groove. Indeed, theoretical models [28, 30] have  
15 shown putative interactions between the p150<sup>Glued</sup> CAP-Gly domain and the C-terminal  
16 peptide of EB1 and TBCB.

17  
18 Taking into account the structural features of the TBCB C-terminal domain, we decided  
19 to go further in understanding the TBCB and TBCB C-terminus interaction and to  
20 determine whether the C-terminal region would also affect the tubulin binding ability of  
21 TBCB. These ideas led us to propose the hypothesis of an autoinhibitory mechanism  
22 where the TBCB C-terminal extension folds over the globular part of its own CAP-Gly  
23 domain and structurally blocks the conserved groove involved in the interaction with  
24 EEY/F-COO<sup>-</sup> elements characteristic of EBs, CLIP-170, and  $\alpha$ -tubulin. For this purpose,  
25 we have cloned the human *Tbcb* gene and constructed two *Tbcb* mutants lacking the last  
26 three (TBCB $\Delta$ 3) and last nine (TBCB $\Delta$ 9) amino acid residues, predicted to be  
27 unstructured. These truncated proteins were overexpressed in HeLa cells and visualized  
28 using new polyclonal anti-TBCB antibodies (see Material and Methods).

29  
30 Previously, we showed that the overexpression of either TBCE or TBCD in human cell  
31 lines leads to the sequestration of free  $\alpha$ - and  $\beta$ -tubulin respectively, leading to massive  
32 microtubule depolymerization [6-8]. On the other hand, murine TBCB overexpression  
33 only leads to a moderate microtubule depolymerization effect, probably because of the  
34 limiting concentrations under TBCB overexpression conditions, of endogenous TBCE  
35 required for the binding and dissociation of the tubulin heterodimer [9].

36  
37 Unpredictably, overexpression of the TBCB $\Delta$ 3 mutant in HeLa cells induced a massive  
38 microtubule destruction effect, comparable only to that observed upon TBCE  
39 overexpression (Fig 1b; [9]). Quantification of the microtubule destruction effect  
40 revealed that at 30 h post transfection, over 60% of the TBCB $\Delta$ 3 positive cells exhibited  
41 no detectable microtubules, while only less than 20% of the overexpressing cells had an  
42 apparently unaffected microtubular cytoskeleton. Similar results were obtained for the  
43 TBCB $\Delta$ 9 mutant. These findings strongly support the proposed idea that TBCB is self-  
44 inhibited by its C-terminus and that the removal of only the last three amino-acid residues  
45 from this domain is sufficient to activate TBCB.

46  
47 These results prompted us to investigate whether TBCB $\Delta$ 3 was able to depolymerize  
48 microtubules assembled in vitro. For this purpose, we purified brain tubulin and the  
49 untagged TBCB $\Delta$ 9 and TBCB $\Delta$ 3 proteins (Fig S1a). Stoichiometric amounts of purified  
50 TBCB $\Delta$ 3 or ovalbumin (negative control) were incubated with GTP and polymerized  
51 purified tubulin. The incubation mix was then centrifuged, and both the soluble and  
52 insoluble fractions were analyzed by SDS-PAGE to determine the amounts of tubulin and  
53  
54  
55  
56  
57  
58

1  
2  
3  
4 TBCB $\Delta$ 3 proteins in the two fractions (Fig S1b). These experiments revealed that  
5 TBCB $\Delta$ 3 was essentially present in the supernatant fractions. Moreover, similar amounts  
6 of tubulin were found in the supernatant and pellet fractions in the presence or absence of  
7 TBCB $\Delta$ 3, which were also similar to those found when ovalbumin was used (Fig S1b).  
8 These results lead to the conclusion that TBCB $\Delta$ 3 is not able to depolymerize  
9 microtubules in vitro, presumably because of the lack of a factor mediating its in vivo  
10 effect.

11  
12  
13 The proposed model for TBCB's autoinhibition implies the interaction of the C-terminal  
14 tail of this cofactor with its own CAP-Gly domain. To test this hypothesis, we performed  
15 quantitative binding assays by using fluorescence polarization of fluorescein labeled  
16 peptides (Table 1; see also Supplementary Material and Supplementary Table 1). The  
17 equilibrium dissociation constants show that the C-terminal nonapeptide (peptide 1)  
18 presents a higher affinity for TBCB (12  $\mu$ M) than that displayed by the same peptide  
19 lacking the last three residues (peptide 2), which was six times lower. Similarly, the C-  
20 terminal deleted proteins TBCB $\Delta$ 3 and TBCB $\Delta$ 9 showed a sixfold reduction in the  
21 affinity for the complete C-terminal peptide of TBCB (peptide 1). Besides, the binding  
22 affinities exhibited by the C-terminal deleted peptide 2 for the deleted TBCB forms are  
23 significantly lower than for the full-length protein. Together these results strongly support  
24 the idea that the last three amino acid residues of the TBCB C-terminus are involved in  
25 the binding to TBCB, thus reinforcing our model of TBCB autoinhibition.

26  
27  
28 Finally, CAP-Gly domains have a high affinity for the C-terminal tail of  $\alpha$ -tubulin (i.e.,  
29 CLIP-170 CAP-Gly domain 2; [31]). In order to corroborate our model, we have also  
30 quantified the binding affinity of TBCB to two different  $\alpha$ -tubulin peptides (Tables 1 and  
31 S1; peptide 3 and peptide 4). We designed a peptide (GEGEEEGEEY) corresponding to  
32 the C-terminus of  $\alpha$ -tubulin isotypes 1 and 2, containing the last tyrosine residue, known  
33 to be critical for binding to CAP-Gly domains [31]. As expected, all three polypeptides  
34 (TBCB, TBCB $\Delta$ 3, and TBCB $\Delta$ 9) displayed a  $K_D$  value higher than that exhibited by the  
35 TBCB-peptide (EEDYGLDEI). In the case of wild-type TBCB and  $\alpha$ -tubulin  
36 (GEGEEEGEEY), the  $K_D$  is about four times higher (43  $\mu$ M) than that obtained for the  
37 TBCB peptide (EEDYGLDEI).

38  
39  
40 Altogether, the results indicate that TBCB does not interact with tubulin dimers and  
41 demonstrate that the TBCB CAP-Gly domain is functionally different from other CAP-  
42 Gly domains. Finally, they confirm that TBCB is autoinhibited by the last three amino  
43 acid residues of its C-terminus.

#### 44 45 46 47 **The C-terminal acidic tail of TBCB is responsible for TBCE interaction**

48  
49  
50 Previous work from our group has shown that when incubated together, purified  
51 mammalian TBCB and TBCE produce a new peak in gel filtration analysis  
52 chromatograms that correspond approximately to the sum of the molecular masses of  
53 individual TBCB and TBCE [9]. Further analysis of this peak revealed the presence of  
54 both cofactors suggesting that purified TBCB forms a binary complex with TBCE ([9]  
55 and Fig 2a, left panel). Bearing in mind these results and that the last three amino acid  
56 residues of the TBCB C-terminus are critical for its activity, we have investigated  
57  
58

1  
2  
3  
4 whether the TBCB $\Delta$ 3 or TBCB $\Delta$ 9 truncated proteins are also able to dimerize with  
5 TBCE. Interestingly, when purified TBCE is incubated with purified TBCB $\Delta$ 3 (Fig 2a,  
6 right panel) no additional peaks are detected in gel filtration chromatograms. Indeed,  
7 chromatograms only revealed peaks corresponding to the species present when the single  
8 purified proteins were analyzed. This observation was confirmed by SDS-PAGE analysis  
9 of the corresponding fractions (Fig 2a). These results strongly suggest that none of the  
10 TBCB C-terminus deleted mutants is able to interact with TBCE and that the last three  
11 amino acid residues of TBCB are essential for the TBCE recognition.  
12  
13

### 14 15 **TBCE and TBCB, the tubulin heterodimer dissociation machine**

16  
17 Because the TBCE and TBCB interaction is required for an efficient tubulin heterodimer  
18 dissociation activity, the results above predict that the last three amino acid residues of  
19 TBCB are also critical for this process. Therefore, we have investigated the tubulin  
20 heterodimer dissociation activity of TBCE in the presence of either full-length TBCB or  
21 TBCB $\Delta$ 3 and have quantified the different molecular species produced by native-PAGE.  
22 When tubulin heterodimers are incubated with TBCE in the presence of TBCB, an extra  
23 band (Fig 2b), which probably corresponds to the ternary complex composed of TBCB,  
24 TBCE, and  $\alpha$ -tubulin, is detected in native gels. To confirm the composition of this band  
25 (Fig 2b, second dimension), we have analyzed the sample where TBCE was incubated  
26 with TBCB and  $\alpha$ -tubulin using a nonclassical two-dimensional PAGE method [23].  
27 Thus the incubation sample was analyzed in a native gel for the first dimension (Fig 2b).  
28 Then, to resolve the complex's composition, the respective lane of the native gel was  
29 directly applied into a denaturing gel for the second dimension. This analysis confirmed  
30 that the new extra band corresponds to the ternary complex (Fig 2b and 2d). Interestingly,  
31 in similar incubations where TBCB was replaced by TBCB $\Delta$ 3, the ternary complex is  
32 absent, and instead an extra band that migrates a little bit less than that corresponding to  
33 tubulin heterodimers was found. To determine the molecular composition of this new  
34 band, we performed a second-dimension analysis similar to that described above (Fig 2c  
35 and 2d). This analysis showed that this band corresponds to the binary complex  
36 containing  $\alpha$ -tubulin and TBCB $\Delta$ 3. Therefore, TBCB $\Delta$ 3 is able to interact with  $\alpha$ -tubulin  
37 but not with TBCE.  
38

39 TBCE and TBCD were characterized as the tubulin cofactors that are able to dissociate  
40 the tubulin heterodimer [6-8]. Although it was stated that TBCB cannot dissociate the  
41 tubulin heterodimer, we decided to investigate whether TBCB or TBCB $\Delta$ 3 or both also  
42 have this ability. For this purpose, we decided to repeat the dissociation experiments by  
43 performing them in the presence of TBCA to improve the visualization of the tubulin  
44 heterodimer dissociation. It was previously shown that this cofactor, capturing the  $\beta$ -  
45 tubulin subunits emerging from tubulin dimers dissociated by TBCE, forms a binary  
46 complex detectable in native gels [8]. As observed in Fig 2d, when tubulin heterodimers  
47 are incubated with TBCE in the presence of TBCB and TBCA, dissociation is complete,  
48 forming the ternary complex (TBCB, TBCE, and  $\alpha$ -tubulin) described above, which  
49 comigrates with TBCA and the binary TBCA and  $\beta$ -tubulin complex. On the other hand,  
50 when TBCE and tubulin heterodimers are incubated with TBCB $\Delta$ 3 instead of TBCB, the  
51  
52  
53  
54  
55  
56  
57  
58

1  
2  
3  
4 ternary complex is not detected, but binary complexes containing TBCB $\Delta$ 3 and  $\alpha$ -  
5 tubulin, and TBCA and  $\beta$ -tubulin are clearly visible. In contrast, neither TBCB nor  
6 TBCB $\Delta$ 3 by itself gives rise to the formation of TBCA and  $\beta$ -tubulin complexes,  
7 demonstrating that they do not have the ability to dissociate the tubulin heterodimer in the  
8 absence of TBCE (Fig 2d).  
9

10 To understand better the role of these cofactors in tubulin heterodimer disruption, we  
11 decided to perform a time course of the dissociation activities of TBCE alone and in the  
12 presence of stoichiometric amounts of TBCB or TBCB $\Delta$ 3. We observed that while TBCE  
13 alone dissociates 60% of the tubulin heterodimers in 30 minutes (Fig 2e), TBCE in the  
14 presence of TBCB is able to dissociate about 90% in less than 30 seconds (the minimal  
15 time required to mix the incubation components and load it into the gel). In contrast, in  
16 the same period, but in the presence of TBCB $\Delta$ 3, only 25% of tubulin heterodimers are  
17 dissociated by TBCE. Although in the presence of TBCE there is a clear difference  
18 between the dissociating activities of the TBCB and the TBCB $\Delta$ 3 (90% to 25%), the  
19 small increase in the dissociation activity percentage in the presence of TBCB $\Delta$ 3  
20 compared with that observed for TBCE alone (9%) might be because TBCB $\Delta$ 3 can form  
21 a binary complex with  $\alpha$ -tubulin that would facilitate the dissociation activity of TBCE  
22 (Fig 2f and 2g).  
23

24 Together, our data clearly show that the last three residues in TBCB are not required for  
25 the formation of the binary complex with  $\alpha$ -tubulin. However, they are not only  
26 implicated in TBCB autoinhibition but also essential for the interaction of TBCB with  
27 TBCE and therefore required for the assembly of an efficient tubulin heterodimer  
28 dissociation machine.  
29

30 Moreover, based on these results, we put forward the hypothesis that TBCE would  
31 interact with the C-terminus of TBCB, which would lead to the derepression of this  
32 cofactor triggering a microtubule catastrophe. However, the observation that neither  
33 TBCB $\Delta$ 3 nor TBCB $\Delta$ 9 (results not shown) is able to interact with TBCE is still puzzling  
34 because their overexpression resulted in massive microtubule depolymerization in HeLa  
35 cells (see Fig 1b and 1c).  
36  
37  
38  
39  
40

### 41 **In solution, TBCB is a monomer as revealed by biophysical studies and cross-** 42 **linking experiments** 43

44 The possible TBCB autoinhibition is supported by the interaction observed between the  
45 C-terminal peptide molecules in the crystal structure of the CAP-Gly domain of *C.*  
46 *elegans* TBCB [26]. To obtain clues regarding the behavior of native TBCB that could  
47 help us to elucidate the molecular mechanism underlying its autorepressed activity, we  
48 used different experimental approaches to investigate whether TBCB is a monomer or a  
49 dimer in solution. For this purpose, we first determined the circular dichroism (CD)  
50 spectra of the TBCB, TBCB $\Delta$ 3, and TBCB $\Delta$ 9 proteins (Supplementary Material). The  
51 CD spectra of the three proteins (Fig S2a, left panels) was characterized by the presence  
52 of two minima at 208 and 217 nm, which are indicative of a mixed population of  $\alpha$ -  
53 helical (20%,  $[\theta]_{222/208} = 0.87$ ) and  $\beta$ -strand (30%) conformations. The absence of a  
54 minimum value at 222 nm (typical of all  $\alpha$  proteins) and a zero crossing (typical of a  $\alpha$ -  
55  
56  
57  
58  
59  
60  
61  
62  
63  
64  
65

1  
2  
3  
4 helices and  $\beta$ -strands) suggest the additional presence of disordered (random coils and  
5 turns) structures (50%).  
6  
7 Subsequently, we decided to study the state of aggregation of these proteins by dynamic  
8 light scattering, but obtained inconclusive results (DLS, [32]; see Supplementary  
9 Material). By using a gel filtration analysis, we have previously characterized the  
10 molecular components of the different complexes formed between TBCB, TBCE, and  
11 tubulin [9]. Based on the elution volumes, the estimated molecular mass of TBCB was  
12 30%–40% larger (40 kDa) than that predicted from its amino acid sequence (27 kDa).  
13 Curiously, this value for TBCB coincided with the molecular mass estimated from its  
14 mobility on SDS-PAGE. However, the apparent molecular mass of the complexes formed  
15 between TBCB and TBCE, and between TBCB and TBCE and  $\alpha$ -tubulin, suggested that  
16 they were the result of the sum of the molecular masses of the monomeric subunits.  
17 These apparent discrepancies in the values of TBCB molecular masses were maintained  
18 upon DLS estimations of the molecular mass of TBCB (69 kDa), TBCB $\Delta$ 3 (53 kDa), and  
19 TBCB $\Delta$ 9 (34 kDa; Fig S2b). In order to clarify these observations, we decided to  
20 investigate the state of oligomerization of the three proteins by cross-linking experiments  
21 (Fig 3a) and analytical ultracentrifugation (Fig 3b). We used glutaraldehyde as a general  
22 protein cross-linker and a protein (EB1) with a very low  $K_D$  for dimer formation, as a  
23 positive control. Interestingly, the results revealed that purified TBCB, as well as  
24 TBCB $\Delta$ 3, migrates in SDS-PAGE as a single band with an apparent molecular mass of  
25 about 38–40 kDa. Nevertheless, when these two proteins are incubated with  
26 glutaraldehyde (0.05%), the band corresponding to 40 kDa, although still visible in trace  
27 amounts, is substituted by a new band corresponding to species with a molecular mass of  
28 about 27 kDa (Fig 3a). This molecular mass is in agreement with the theoretical  
29 molecular mass of these two proteins. On the other hand, the EB1 control protein, which  
30 normally migrates as a single band of 32–34 kDa after glutaraldehyde treatment, migrates  
31 as a band of 64 kDa, which is consistent with its size in gel filtration experiments (Fig  
32 S2d). These results were confirmed by an analytical ultracentrifugation analysis that was  
33 performed at 20°C at 160,000  $\times g$  (Fig 3b). Indeed, the analytical ultracentrifugation  
34 showed that the molecular mass of TBCB was  $\sim$ 25.5 kDa, corresponding to the size of  
35 the monomer (27 kDa). Taken together, all these results led us to conclude that TBCB  
36 behaves as a monomer and to suggest that its self-inhibition occurs within the same  
37 molecule and not between two or more TBCB molecules.  
38  
39  
40  
41  
42  
43  
44  
45

### 46 **TBCB localizes to the centrosome and mitotic spindle microtubules**

47  
48 TBCB has been shown to colocalize with Pak1 protein on newly polymerized  
49 microtubules [13]. Because the overexpression of TBCB and TBCB $\Delta$ 3 leads to  
50 microtubule depolymerization, we decided to investigate the subcellular distribution of  
51 the overexpressed YFP:TBCB protein in HeLa cells throughout the cell cycle.  
52 As observed for the wild-type endogenous protein [9], YFP:TBCB is mostly a soluble  
53 cytoplasmic protein in interphase cells (Fig 4a). A prominent spot of YFP:TBCB is often  
54 localized at the centrosome (double spot) and at the base of the primary cilium (Fig 4B).  
55 Indeed, the distribution of YFP:TBCB during mitosis revealed two clear YFP:TBCB  
56 spots at prophase (Fig 4a, top middle). Interestingly, as mitosis progressed toward  
57  
58  
59  
60  
61  
62  
63  
64  
65

1  
2  
3  
4 metaphase, TBCB was also localized to spindle microtubules (Fig 4a, top right). This  
5 localization was also observed for overexpressed wild-type untagged TBCB by  
6 immunostaining and is in accordance with previous analyses performed for endogenous  
7 TBCB in human and mouse cells [9,13,33]. Furthermore, with this new analysis, we  
8 observed that during anaphase A, YFP:TBCB becomes more visible as thin filaments  
9 bridging the midzone, and by anaphase B most of this cofactor had progressively  
10 disappeared from the centrosome and was concentrated on the midbody microtubules  
11 (Fig 4a, bottom). At the end of telophase, TBCB was apparently absent from the  
12 centrosome, concentrating in a unique spot at the midbody. These localization results  
13 show evidence that TBCB can bind to microtubules. However, we know from all the  
14 results described above that TBCB cannot recognize tubulin heterodimers, suggesting  
15 this binding to be indirect, occurring through the interaction of TBCB with a microtubule  
16 binding protein.  
17  
18  
19  
20

### 21 **TBCB $\Delta$ 3 interacts with EB1 and the cytosolic chaperonin CCT**

22  
23 That in vivo TBCB is able to localize at mitotic spindle microtubules and to promote  
24 microtubule destabilization, whereas in vitro it is not able to depolymerize or even to  
25 interact with microtubules, strongly suggests that in vivo TBCB should have an  
26 interactor(s) that mediates its functions toward microtubules. This prompted us to search  
27 for TBCB molecular interactors. In a first approach, we have performed different  
28 experiments such as yeast two-hybrid and immunoprecipitation techniques, but we were  
29 unsuccessful in the identification of any TBCB interactor. This could be ascribed to the  
30 fact that we have not used specific conditions required to avoid disruption of weak  
31 interactions. To overcome these problems, we constructed an affinity column with bound  
32 recombinant untagged TBCB $\Delta$ 3, the derepressed version of TBCB. Bound proteins or  
33 complexes were specifically eluted with a salt gradient that produced a double peak  
34 between 100 and 200 mM NaCl, and the corresponding fractions were analyzed by SDS-  
35 PAGE.  
36  
37  
38

39 The different bands (Nos. 1–6, Fig 5b) detected in SDS-PAGE gels were subjected to  
40 trypsin digestion followed by mass fingerprinting analysis. Notably, this analysis  
41 revealed that band No. 1 corresponds to human EB1. The sequence coverage was 83%  
42 corresponding to MARE 1 (UniProt accession C1BKD9, Fig S3A). The analysis showed  
43 that band Nos. 3–5 correspond to the eight distinct human CCT subunits required to  
44 assemble CCT completely. All the CCT-subunits were identified with a sequence  
45 coverage higher than 45%, and for most of the cases, the coverage was about 70% (Fig  
46 S4a). The presence of complete CCT hetero-oligomeric particles in the eluted fractions  
47 was also confirmed by conventional electron microscopy. Notably, CCT is a group II  
48 chaperonin mostly committed to the folding of actins and monomeric  $\alpha$ - and  $\beta$ -tubulin  
49 [34]. Therefore, this is the first evidence demonstrating that a tubulin folding cofactor is  
50 able to bind directly to CCT, an interaction that may be relevant for the tubulin folding  
51 process.  
52  
53  
54

55 In addition to these interactors, we also found that band No. 2 corresponds to  $\alpha$ - and  $\beta$ -  
56 tubulin (Fig 5b). In fact, five  $\alpha$ -tubulin isotypes and seven  $\beta$ -tubulin isotypes (Fig S4b)  
57 were unequivocally identified with a sequence coverage for all isotypes higher than 20%  
58  
59  
60  
61  
62  
63  
64  
65

1  
2  
3  
4 and generally with a value of about 50%–60% (Fig S4b). These results also show that the  
5 HEK293 cell line expresses all known tubulin isotypes. Because TBCBΔ3 does not bind  
6 tubulin heterodimers or microtubules in vitro and only binds to α-tubulin, but not to β-  
7 tubulin monomers, these results strongly suggest that TBCBΔ3 would bind microtubules  
8 through a partner and that this partner must be EB1.  
9

### 10 **EB1 overexpression prevents TBCBΔ3 microtubule destruction**

11  
12  
13  
14 The finding that EB1 is a TBCB interactor makes this protein the most attractive  
15 candidate for explaining how TBCB is able to regulate microtubule dynamics. Because  
16 EB1 is known to stabilize the plus ends of microtubules, its interaction with TBCB would  
17 explain how TBCB is able to promote a microtubule catastrophe when overexpressed. In  
18 this context, we may expect that TBCB has the ability to sequester EB1 from microtubule  
19 plus ends. If these hypotheses were true, the overexpression of EB1 would be sufficient  
20 to rescue the observed phenotype of microtubule depolymerization when TBCB and  
21 TBCBΔ3 are overexpressed. This would also provide evidence of the interaction of EB1  
22 with TBCB in vivo. To examine this model, we have cotransfected HeLa cells with wild-  
23 type TBCB and GFP:EB1 or TBCBΔ3 and GFP:EB1. As predicted, the obtained results  
24 show that microtubule destruction resulting from simultaneous overexpression of  
25 TBCBΔ3 + GFP:EB1 or TBCB and GFP:EB1 was substantially less accentuated than  
26 that observed in cells only overexpressing TBCBΔ3 or TBCB, respectively (Fig 6a). We  
27 also observed that the typical GFP:EB1 comets, resulting in the localization of this  
28 protein at growing microtubule plus ends, were no longer observable (Fig 6a, bottom),  
29 suggesting that excess TBCBΔ3 was interacting with EB1 modifying its intracellular  
30 distribution.  
31

32  
33  
34  
35 To confirm further whether TBCBΔ3 interacts with EB1 in this system, we next  
36 quantified and compared the microtubule destruction effect at specific time points against  
37 the background of overexpressing GFP:EB1+TBCBΔ3 versus overexpressing  
38 GFP:EB1+TBCB. Therefore, cotransfected cells and controls were fixed at different time  
39 points. Triple labeling experiments revealed that 10 times as many cells preserved their  
40 microtubule cytoskeleton when cotransfected with both genes (Fig 6b). Hence, this  
41 system suggests that the TBCBΔ3 depolymerization effect is virtually blocked by  
42 overexpressed EB1 and thus confirms that TBCBΔ3 and EB1 interact in vivo.  
43  
44  
45  
46

### 47 **Discussion**

48  
49  
50 In this work, we found that the TBCB CAP-Gly domain is autoinhibited by interaction  
51 with the last three residues of its C-terminus. Our data also show that these last three  
52 residues of TBCB are required for TBCE recognition, interaction and tubulin heterodimer  
53 dissociation. Therefore, we have proposed a molecular mechanism explaining how TBCB  
54 and TBCE form a binary complex that efficiently recognizes and dissociates the tubulin  
55 heterodimer.  
56

57 Biophysical studies revealed that a TBCB protein lacking the last three amino acid  
58 residues (TBCBΔ3) behaves as the wild-type protein with a similar CD spectrum and  
59  
60  
61  
62  
63  
64  
65

1  
2  
3  
4 response to unfolding by heat. Cross-linking experiments and analytical  
5 ultracentrifugation, in contrast to dynamic light scattering, show that TBCB behaves as a  
6 monomer of 25.5 kDa. The TBCBA9 protein, which lacks the last nine amino acid  
7 residues, presents a similar CD spectrum and the same unfolding temperature as TBCB  
8 and TBCBA3. This truncated version of the TBCB protein shows a completely different  
9 behavior under heat denaturing conditions, but the values from the dynamic light  
10 scattering also suggest that it is a monomer (Fig S2). When overexpressed in human cells,  
11 TBCB is able to induce microtubule loss [9]. Although initially this could be ascribable  
12 to its interaction with endogenous TBCE, we found that the mutant lacking the last three  
13 amino acid residues and unable to interact with TBCE depolymerizes microtubules in  
14 vivo with a higher efficiency. This suggests that the C-terminal region is an  
15 autoinhibitory sequence and that the mechanism of microtubule depolymerization by  
16 TBCBA3 is TBCE independent (Fig 7a). Microtubule destruction was accompanied by an  
17 intense tubulin background in the cells when detected with both anti- $\alpha$ - and anti- $\beta$ -  
18 tubulin antibodies, suggesting the presence of soluble tubulin heterodimers in the cytosol  
19 of the cells. This cytoplasmic background is very unusual in TBCE or TBCD  
20 overexpressing cells where these two cofactors sequester either  $\alpha$ - or  $\beta$ -tubulin  
21 respectively upon tubulin heterodimer dissociation, which leads to microtubule  
22 depolymerization and microtubule network collapse.

23  
24 To gain insights into the mechanism by which TBCB causes microtubule  
25 depolymerization, we have studied whether or not TBCB was able to depolymerize  
26 microtubules assembled in vitro. We demonstrated that TBCB was not a microtubule  
27 depolymerizing enzyme in itself (Fig S1b), which led us to propose the hypothesis of the  
28 existence of a TBCB partner that would be implicated in the TBCB microtubule  
29 depolymerization mechanism. Specifically, we proposed that TBCBA3 was derepressed  
30 on its presumed ability to bind to a partner through which it would promote microtubule  
31 depolymerization. For this reason, we decided to construct an affinity column containing  
32 the derepressed version of TBCB. The reasoning behind the use of the derepressed TBCB  
33 mutant was to increase the possibility of identifying partners that would not be easy to  
34 discover with the wild-type repressed protein.

35  
36 Therefore, we have performed TBCBA3 affinity binding studies by constructing an  
37 affinity column with this polypeptide bound to a matrix and incubating it with a soluble  
38 human cell protein extract. Our results show that this derepressed TBCB protein was able  
39 to interact with Hsp90, CCT, and EB1. Indeed, the amount of Hsp90 that appears to be  
40 bound to the affinity column containing TBCBA3 was low compared with EB1 and CCT.  
41 Consequently, and although this interaction has a putative role, we did not continue  
42 studying this interaction. The same was true for CCT, although we can envisage an  
43 important role for the CCT-TBCB interaction in the process of CCT-mediated  $\alpha$ -tubulin  
44 folding.

### 45 46 47 48 49 50 51 52 53 54 **Model of TBCB-mediated $\alpha$ -tubulin folding bound to CCT**

55  
56 The establishment that CCT is one of the interactors of TBCB, as revealed by the use of  
57 the affinity column (Fig 5) adds new data to the model of how proper tubulin folding and  
58 dimerization may occur in vivo. This is the first time that a tubulin folding cofactor was  
59



1  
2  
3  
4 found to associate with this chaperonin. The possibility of TBCB being a CCT substrate  
5 was excluded because TBCB interacts with CCT while binding  $\alpha$ -tubulin [9]. This  
6 strongly suggests that the interaction of TBCB with CCT might contribute for the proper  
7 tubulin folding and dimerization. The interaction of TBCB with CCT is also supported by  
8 the fact that after incubation of different amounts of TBCB with purified bovine CCT, an  
9 extra band with a higher molecular mass than those corresponding to CCT or TBCB was  
10 recognized by anti-TBCB antiserum (our unpublished results). This band migrates at the  
11 same position as the extra band containing CCT,  $\alpha$ -tubulin, and TBCB previously  
12 observed to occur in in vitro translation assays [9]. Together, these results led us to  
13 propose a model in which TBCB would recognize  $\alpha$ -tubulin bound to CCT (Fig 7b). It  
14 has been shown in vitro and in vivo that free  $\alpha$ - or  $\beta$ -tubulin will aggregate in the absence  
15 of a partner (the other tubulin partner or tubulin cofactors, [4,5]). Therefore, our proposed  
16 mechanism predicts that  $\alpha$ -tubulin would be released from CCT bound to TBCB ensuring  
17 that the  $\alpha$ -tubulin monomer would never aggregate. Later, the monomeric tubulin subunit  
18 would be transferred to TBCE for dimer assembly and incorporation into growing  
19 microtubules or would be transferred to the degradative pathway involving the  
20 proteasome if not properly folded [35].  
21  
22  
23  
24  
25

### 26 **Model of TBCB-mediated microtubule depolymerization**

27  
28  
29 Previous studies have shown that TBCB is regulated by phosphorylation being a substrate  
30 of Pak1 as revealed in a yeast two-hybrid screen. Pak1 directly phosphorylates TBCB,  
31 and both proteins colocalize on newly polymerized microtubules [13]. We have also  
32 shown that the YFP:TBCB protein colocalizes with microtubules of the mitotic spindle,  
33 and as mitosis progresses, the staining gradually increases in microtubules of the spindle  
34 midzone where active polymerizing microtubules are present. Moreover, TBCB depletion  
35 in neuronal cells by siRNA induces axonal extension and growth cone detachment  
36 suggesting a role for TBCB at microtubule tips [33]. Recently, TBCB was identified as a  
37 target for nitrogen-containing bisphosphonates (N-BP), drugs extensively used in the  
38 treatment of bone diseases. In fact, TBCB is upregulated in mammalian cells after N-BP  
39 treatment inducing the loss of microtubule architecture in sites of active microtubule  
40 assembly, such as neuronal protrusions [36]. This effect might be explained by the  
41 observation that overexpression of TBCB in growth cones leads to microtubule  
42 depolymerization [33].  
43  
44

45  
46 EBs proteins are dimeric proteins formed by two functional domains [37]. The N-  
47 terminal domain mediates microtubule binding, while the C-terminal domain has a coiled  
48 coil responsible for dimerization and an unstructured tail (Fig 7c). Several models have  
49 been proposed to explain EB binding to the plus end of microtubules. Crystal structures  
50 of the C-terminal domain of EB1 and the CAP-Gly domains of the dynactin subunit  
51 p150<sup>Glued</sup> led Hayashi and coworkers [38] to postulate that EB1 is autoinhibited and that  
52 this conformation is unhampered by binding of a CAP-Gly-containing protein (p150<sup>Glued</sup>,  
53 Fig 7c). Although TBCB and TBCE contain a CAP-Gly domain, these proteins were  
54 never described as localizing at microtubule tips as other +TIPs proteins. TBCE was also  
55 a good candidate for such a role, but we could not see interaction with EB1 in vitro.  
56 While the model proposed by Hayashi and coworkers [38] is well supported by the  
57  
58  
59  
60  
61  
62  
63  
64  
65

1  
2  
3  
4 different structures solved (Fig 7), the mechanism by which EBs bind to microtubules  
5 remains unclear. Although the removal of the EB tail blocked, as predicted, binding to  
6 partners [39], it had no effect in vivo on microtubule plus-end accumulation. Also,  
7 removal of the C-terminal tail of EBs does not alter the global conformation of the  
8 protein [40], which does not support the model proposed by Hayashi and coworkers [38].  
9 In addition, Buey and colleagues (40) suggested that the negative charge of the domain is  
10 responsible for the specificity of the EBs to the microtubule tip. Despite the different  
11 models that try to explain the preference of EB proteins for the growing microtubule plus  
12 end, it seems that EBs recognize an inaccessible region of tubulin in the GTP bound form  
13 [41]. It is thought that the binding of EBs to microtubule tips is dynamic, being  
14 characterized by rounds of binding and unbinding [19]. Although we detected an  
15 interaction of TBCB with EB1, in vivo and using our polyclonal antibodies against  
16 human or murine TBCB, we never found typical EB-comets. TBCB is a CAP-Gly-  
17 containing protein, but when we performed double immunolabeling with GFP-EB1 and  
18 TBCB we could not colocalize TBCB to the microtubule tips that were clearly seen for  
19 EB1. For this reason, it was surprising to find that EB1 was one of the major interactors  
20 of TBCB. Thus, we decided to study the in vitro interaction of TBCB with EB1 using  
21 purified untagged proteins. Unexpectedly, we found no interaction under the conditions  
22 tested (Fig S2d). We could not rule out the possibility that specific posttranslational  
23 modifications in the EB1 protein were required for TBCB binding. This would not be the  
24 case for TBCB because the protein used in the affinity column was purified from *E. coli*  
25 and could not have posttranslational modifications. The detailed mass spectrometric  
26 analysis of the EB1 polypeptide showed an acetylation at alanine-2 (Fig S3a). This  
27 cotranslational acetylation occurrence takes place only in eukaryotes. This usual  
28 modification probably does not add functional diversity to the EB1 polypeptide,  
29 supporting the notion that TBCB and EB1 do not interact unless EB1 is derepressed. We  
30 isolated microtubule fragments containing different  $\alpha$ - and  $\beta$ -tubulin polypeptides (Fig  
31 S4b) bound to TBCB. In our experiments ([9] and this work), TBCB did not interact  
32 along the microtubule, although we cannot rule out an interaction with microtubule ends.  
33 That we could isolate microtubule fragments with bound EB1 provided us with strong  
34 evidence that TBCB $\Delta$ 3 binds and sequesters EB1 from microtubule ends leading to  
35 microtubule depolymerization [42].

36 We have established that the C-terminal peptide of TBCB is required for binding to  
37 TBCE and for efficient tubulin heterodimer dissociation (Fig 2). TBCB also recognizes  
38 EB1 at the plus end of the microtubule, and our results suggest that this interaction takes  
39 place when EB1 is also derepressed, probably after interaction with another +TIP protein  
40 or after binding to microtubules.

41 Finally, we have also demonstrated that cotransfection with EB1 prevents TBCB $\Delta$ 3  
42 microtubule destruction and that cells recover their normal phenotype, confirming that  
43 TBCB $\Delta$ 3 and EB1 interact in vivo. This is more than sufficient to justify microtubule  
44 destabilization, but, as TBCB forms an active heterodimer with TBCE in tubulin  
45 dissociation, we suggest that this is also the mechanism by which these proteins regulate  
46 microtubule dynamics (Fig 7c).

47 In this way, TBCB participates in microtubule dynamics, and as shown here, the  
48 deregulation of TBCB activity induces a microtubule catastrophe in living cells.

## Acknowledgments

This study was funded by BFU2007-64882, BFU2008-01344 and BFU2010-18948, the Consolider-Ingenio Spanish Ministry of Education and Science Centrosome-3D and the Instituto de Formación e Investigación Marqués de Valdecilla. The funders had no role in study design, data collection and analysis, decision to publish, or preparation of the manuscript. We thank Laura Alvarez and Begoña Ubilla for excellent technical assistance. Mass spectrometry analysis was performed in the Proteomics Core Facility-SGIKER, member of ProteoRed, at the University of the Basque Country. Supplementary information is available at The EMBO Journal Online

## Conflict of interest

None of the authors have a financial interest related to this work.

## References

1. Desai A, Mitchison TJ (1997) Microtubule polymerization dynamics. *Annu Rev Cell Biol* 13: 83-117
2. Amos LA (2000) Focusing-in on microtubules. *Curr Opin Struct Biol* 10: 236-241
3. Li H, DeRosier DJ, Nicholson WV, Nogales E, Downing KH (2002a) Microtubule structure at 8 Å resolution. *Structure* 10: 1317-1328
4. Lewis SA, Tian G, Cowan NJ (1997) The alpha- and beta-tubulin folding pathways. *Trends Cell Biol* 12: 479-484
5. López-Fanarraga M, Avila J, Guasch A, Coll M, Zabala JC (2001) Review: postchaperonin tubulin folding cofactors and their role in microtubule dynamics. *J Struct Biol* 135: 219-229
6. Bhamidipati A, Lewis SA, Cowan NJ (2000) ADP ribosylation factor-like protein 2 (Arl2) regulates the interaction of tubulin-folding cofactor D with native tubulin. *J Cell Biol* 149: 1087-1096
7. Martín L, Fanarraga ML, Aloria K, Zabala JC (2000) Tubulin folding cofactor D is a microtubule destabilizing protein. *FEBS Lett* 470: 93-95
8. Kortazar D, Carranza G, Bellido J, Villegas JC, Fanarraga ML, Zabala, JC (2006) Native tubulin-folding cofactor E purified from baculovirus-infected Sf9 cells dissociates tubulin dimers. *Protein Expr Purif* 49: 196-202
9. Kortazar D, Fanarraga ML, Carranza G, Bellido J, Villegas JC, Avila J, Zabala JC (2007) Role of cofactors B (TBCB) and E (TBCE) in tubulin heterodimer dissociation. *Exp Cell Res* 313: 425-436
10. Feierbach B, Nogales E, Downing KH, Stearns T (1999) Alf1p, a CLIP-170 domain-containing protein, is functionally and physically associated with alpha-tubulin. *J Cell Biol* 144: 113-124
11. Parvari R, Hershkovitz E, Grossman N, Gorodischer R, Loeys B, Zecic A, Mortier G, Gregory S, Sharony R, Kambouris M, Sakati N, Meyer BF, Al Aqeel AI, Al Humaidan AK, Al Zahrani F, Al Swaid A, Al Othman J, Diaz GA, Weiner R, Khan KT, Gordon R, Gelb BD,HRD/Autosomal Recessive Kenny-Caffey Syndrome Consortium (2002) Mutation of TBCE causes hypoparathyroidism-retardation-dysmorphism and autosomal recessive Kenny-Caffey syndrome. *Nat Genet* 32: 448-452
12. Martin N, Jaubert J, Gounon P, Salido E, Haase G, Szatanik M, Guénet JL (2002) A missense mutation in Tbce causes progressive motor neuropathy in mice. *Nat Genet* 32: 443-447
13. Vadlamudi RK, Barnes CJ, Rayala S, Li F, Balasenthil S, Marcus S, Goodson HV, Sahin AA, Kumar R (2005) p21-activated kinase 1 regulates microtubule dynamics by phosphorylating tubulin cofactor B. *Mol Cell Biol* 25: 3726-3736

- 1  
2  
3  
4 14. Tian G, Jaglin XH, Keays DA, Francis F, Chelly J, Cowan NJ (2010) Disease-associated mutations in  
5 TUBA1A result in a spectrum of defects in the tubulin folding and heterodimer assembly pathway. *Hum*  
6 *Mol Genet* 19: 3599-3613
- 7 15. Martins-de-Souza D, Gattaz WF, Schmitt A, Rewerts C, Maccarrone G, Dias-Neto E, Turck CW  
8 (2009) Prefrontal cortex shotgun proteome analysis reveals altered calcium homeostasis and immune  
9 system imbalance in schizophrenia. *Eur Arch Psychiatry Clin Neurosci* 259: 151-63
- 10 16. Wang W, Ding J, Allen E, Zhu P, Zhang L, Vogel H, Yang Y (2005) Gigaxonin interacts with tubulin  
11 folding cofactor B and controls its degradation through the ubiquitin-proteasome pathway. *Curr Biol* 15:  
12 2050-2055
- 13 17. Schuyler SC, Pellman D (2001) Microtubule “plus end tracking proteins”: The end is just the  
14 beginning. *Cell* 105: 421-424
- 15 18. Akhmanova A, Hoogenrad CC (2005) Microtubule plus end-tracking proteins: mechanisms and  
16 functions. *Curr Opin Cell Biol* 17: 47-54
- 17 19. Galjart N (2010) Plus-end-tracking proteins and their interactions at microtubule ends. *Curr Biol* 20:  
18 R528-537
- 19 20. Yu KL, Keijzer N, Hoogenraad CC, Akhmanova A (2011) Isolation of Novel +TIPs and Their Binding  
20 Partners Using Affinity Purification Techniques. *Methods Mol Biol*. 777: 293-316
- 21 21. Llosa M, Aloria K, Campo R, Padilla R, Avila J, Sánchez-Pulido L, Zabala JC (1996) The beta-tubulin  
22 monomer release factor (p14) has homology with a region of the DnaJ protein. *FEBS Lett* 397: 283-289
- 23 22. Zabala JC, Cowan NJ (1992) Tubulin dimer formation via the release of alpha- and beta-tubulin  
24 monomers from multimolecular complexes. *Cell Motil Cytoskel* 23: 222-230
- 25 23. Fanarraga ML, Carranza G, Castaño R, Nolasco S, Avila J, Zabala JC (2010). Nondenaturing  
26 electrophoresis as a tool to investigate tubulin complexes *Methods Cell Biol* 95: 59-75
- 27 24. Lajoie-Mazenc I, Tollon Y, Detraves C, Julian M, Moisand A, Gueth-Hallonet C,  
28 Debec A, Salles-Passador I, Puget A, Mazarguil H (1994) Recruitment of antigenic gamma-tubulin during  
29 mitosis in animal cells: presence of gamma-tubulin in the mitotic spindle. *J Cell Sci* 107: 2825-2837
- 30 25. Avila J, Soares H, Fanarraga ML, Zabala JC (2008) Isolation of microtubules and microtubule proteins.  
31 *Current Protocols in Cell Biology*, John Wiley & Sons Inc (ed) . Malden, MA, USA, pp 3.29.1-3.29.28
- 32 26. Li S, Finley J, Liu ZJ, Qiu SH, Chen H, Luan CH, Carson M, Tsao J, Johnson D, Lin G, Zhao J,  
33 Thomas W, Nagy LA, Sha B, DeLucas LJ, Wang BC, Luo M (2002b) Crystal structure of the cytoskeleton-  
34 associated protein glycine-rich (CAP-Gly) domain. *J Biol Chem* 277: 48596-48601
- 35 27. Weisbrich A, Honnappa S, Jaussi R, Okhrimenko O, Frey D, Jelesarov I, Akhmanova A, Steinmetz,  
36 MO (2007) Structure-function relationship of CAP-Gly domains. *Nat Struct Mol Biol* 14: 959-967
- 37 28. Honnappa S, Okhrimenko O, Jaussi R, Jawhari H, Jelesarov I, Winkler FK, Steinmetz MO (2006) Key  
38 interaction modes of dynamic +TIP networks. *Mol Cell* 23: 663-671
- 39 29. Kaur H, Garg A, Raghava GP (2007) PEPstr: A de novo method for tertiary structure prediction of  
40 small bioactive peptides. *Protein Pept Lett* 14: 626-30
- 41 30. Steinmetz MO, Akhmanova (2008) A Capturing protein tails by CAP-Gly domains. *Trends Biochem*  
42 *Sci* 33: 535-545
- 43 31. Mishima M, Maesaki R, Kasa M, Watanabe T, Fukata M, Kaibuchi K, Hakoshima T (2007) Structural  
44 basis for tubulin recognition by cytoplasmic linker protein 170 and its autoinhibition. *Proc Natl Acad Sci U*  
45 *S A* 104: 10346-10351
- 46 32. Borgstahl GE (2007) How to use dynamic light scattering to improve the likelihood of growing  
47 macromolecular crystals. *Methods Mol Biol* 363:109-129
- 48 33. Lopez-Fanarraga. M, Carranza G, Bellido J, Kortazar D, Villegas JC, Zabala JC (2007) Tubulin  
49 cofactor B plays a role in the neuronal growth cone. *J Neurochem* 100: 1680-1687
- 50 34. Muñoz IG, Yébenes H, Zhou M, Mesa P, Serna M, Park AY, Bragado-Nilsson E, Beloso A, de Cárcer  
51 G, Malumbres M, Robinson CV, Valpuesta JM, Montoya G (2011) Crystal structure of the open  
52 conformation of the mammalian chaperonin CCT in complex with tubulin. *Nat Struct Mol Biol* 18: 14-19
- 53 35. Voloshin O, Gocheva Y, Gutnick M, Movshovich N, Bakhrat A, Baranes-Bachar K, Bar-Zvi D, Parvari  
54 R, Gheber L, Raveh D (2010) Tubulin chaperone E binds microtubules and proteasomes and protects  
55 against misfolded protein stress. *Cell Mol Life Sci* 67: 2025-2038
- 56 36. Bivi N, Romanello M, Harrison R, Clarke I, Hoyle DC, Moro L, Ortolani F, Bonetti A, Quadrifoglio F,  
57 Tell G, Delneri D (2009) Identification of secondary targets of N-containing bisphosphonates in  
58

1  
2  
3  
4 mammalian cells via parallel competition analysis of the barcoded yeast deletion collection. *Genome Biol*  
5 10: R93  
6 37. Akhmanova A, Steinmetz MO (2008) Tracking the ends: a dynamic protein network controls the fate  
7 of microtubule tips. *Nat Rev Mol Cell Biol* 9: 309-322  
8 38. Hayashi I, Wilde A, Mal TK, Ikura M (2005) Structural basis for the activation of microtubule  
9 assembly by the EB1 and p150<sup>Glued</sup> complex. *Mol Cell* 19: 449-460  
10 39. Komarova Y, Lansbergen G, Galjart N, Grosveld F, Borisy GG, Akhmanova A (2005) EB1 and EB3  
11 control CLIP dissociation from the ends of growing microtubules. *Mol Biol Cell* 16: 5334-5345  
12 40. Buey RM, Mohan R, Leslie K, Walzthoeni T, Missimer JH, Menzel A, Bjelic S, Bargsten K, Grigoriev  
13 I, Smal I, Meijering E, Aebersold R, Akhmanova A, Steinmetz MO (2011) Insights into EB1 structure and  
14 the role of its C-terminal domain for discriminating microtubule tips from the lattice. *Mol Biol Cell* 22:  
15 2912-2923  
16 41. Akhmanova A, Steinmetz MO (2011) Microtubule End Binding: EBs Sense the Guanine Nucleotide.  
17 *Curr Biol* 21:R283-R285  
18 42. Tirnauer JS, Grego S, Salmon ED, Mitchison TJ (2002) EB1-microtubule interactions in *Xenopus* egg  
19 extracts: role of EB1 in microtubule stabilization and mechanisms of targeting to microtubules. *Mol Biol*  
20 *Cell* 13: 3614-3626  
21  
22

## 23 **Legends to figures**

### 24 **Figure 1. TBCB is an autoinhibitory protein**

25  
26 a) Schematic drawing of human TBCB depicting the three characterized (UBL, coiled-  
27 coil and CAP-Gly) domains. The UBL domain (green) corresponds to PDB ID, 1V6E  
28 (UBL of murine TBCB), and the CAP-Gly domain (blue) to PDB ID, 1TOV (CAP-Gly  
29 domain of F53f4.3, [26]). In light blue are the corresponding residues that form the  
30 conserved groove in p150<sup>Glued</sup>, interacting with the C-terminal peptide of  $\alpha$ -tubulin [30,  
31 31]. The last nine residues, which are present in the solved domain of F53f4.3, are shown  
32 in red. All structures were drawn using Pymol software (<http://www.pymol.org>).  
33  
34 b) Confocal microscopy projection image of TBCB $\Delta$ 3 overexpression on HeLa cells.  
35 TBCB $\Delta$ 3 (green) produces conspicuous microtubule destruction (white arrow). Moderate  
36 TBCB $\Delta$ 3 levels also severely affect the microtubule cytoskeleton. A high cytoplasmic  
37 tubulin background is observed in these two cells.  
38  
39 c) Statistical analysis of the percentages of cells containing normal, abnormal or absent  
40 microtubules in TBCE, TBCB, and TBCB $\Delta$ 3 overexpressing HeLa cells. A highly  
41 significant increase in cells containing a completely destroyed microtubular cytoskeleton  
42 is observed when the TBCB $\Delta$ 3 mutant (asterisk) is overexpressed compared with wild-  
43 type TBCB. See also Figure S1.  
44  
45  
46  
47  
48

### 49 **Figure 2. Biochemical studies of TBCB $\Delta$ 3**

50 a) TBCB $\Delta$ 3, in contrast to complete TBCB, does not form a binary complex with TBCE.  
51 Plots of A<sub>280</sub> absorbance against elution volume from the size-exclusion chromatography  
52 experiments. The elution profiles of TBCB, TBCB $\Delta$ 3, TBCE, and the interaction of these  
53 proteins were analyzed by gel filtration through a Superdex 200 PC 3.2/30 column (GE-  
54 Healthcare). Three plots are shown: TBCB and TBCB $\Delta$ 3 alone (blue), TBCE alone (red),  
55 and the combination of TBCB and TBCE or TBCB $\Delta$ 3 and TBCE (green). Fractions were  
56  
57  
58  
59  
60  
61  
62  
63  
64  
65

1  
2  
3  
4 subjected to SDS-PAGE. The final concentrations used were 18  $\mu\text{M}$  for TBCE and 15  
5  $\mu\text{M}$  for TBCB and TBCBA $\Delta$ 3.

6  
7 b) and c) Nonclassical two-dimensional native SDS-PAGE of complexes formed in  
8 tubulin dissociation experiments. Aliquots of TBCB (b) or TBCBA $\Delta$ 3 (c) and TBCE and  
9 tubulin heterodimers were incubated at 30°C for 30 min and loaded onto a 6% native  
10 minigel (1D). C, control of tubulin heterodimers; C1, TBCBA $\Delta$ 3; C2, tubulin dissociation  
11 in the presence of TBCE and TBCBA $\Delta$ 3 for 30 min. Bands containing this first dimension  
12 were excised from the gel and loaded onto an 8.5% SDS-polyacrylamide gel as described  
13 in Experimental procedures (2D). After electrophoresis, the gels were stained with  
14 Coomassie Blue. The second dimension (2D) shows the molecular compositions of the  
15 ternary complex in panel b (TBCE, TBCB, and  $\alpha$ -tubulin) and of the binary complex  
16 (TBCBA $\Delta$ 3 and  $\alpha$ -tubulin) in panel c.

17  
18 d) TBCB and TBCBA $\Delta$ 3 do not dissociate the tubulin heterodimer. Aliquots containing  
19 TBCB or TBCBA $\Delta$ 3 were incubated at 30°C for 30 min with tubulin heterodimers in the  
20 presence and absence of TBCE and in the presence of TBCA. The drawing on the right  
21 shows the migration of the different proteins and complexes.

22  
23 e) TBCE slowly dissociates the tubulin heterodimer. Time-course of tubulin dissociation  
24 in the presence of stoichiometric amounts of TBCE. C, control of tubulin heterodimers  
25 incubated for 30 min. Samples were frozen in dry ice until they were loaded into the  
26 native gel.

27  
28 f) TBCE/TBCB, the tubulin dimer dissociation machine. Time-course of tubulin  
29 dissociation in the presence of TBCE and stoichiometric amounts of TBCB or TBCBA $\Delta$ 3.  
30 C1, TBCB; C2, TBCBA $\Delta$ 3; C3, control of tubulin heterodimers; C4, tubulin dissociation in  
31 the presence of TBCE for 30 min. After times indicated, samples were frozen on dry ice  
32 until they were loaded into the native gel. The drawing on the right shows the migration  
33 of the different proteins and complexes. Final concentrations used were 3  $\mu\text{M}$  for tubulin,  
34 2.5  $\mu\text{M}$  for TBCE, and 2.5  $\mu\text{M}$  for TBCB and TBCBA $\Delta$ 3.

35  
36 g) Quantification of tubulin dissociation by TBCE/TBCB and TBCE/TBCBA $\Delta$ 3.  
37 Quantification of the proportions of tubulin dissociation in the experiment shown in e and  
38 f (time 0) using ImageJ software. Data were analyzed using SigmaPlot software.  
39 Experiments were performed in triplicate, and the graph reports the mean  $\pm$  the standard  
40 deviation.  
41  
42  
43  
44

### 45 Figure 3. Biophysical studies of TBCB and TBCBA $\Delta$ 3

46  
47 a) Cross-linking of TBCB and TBCBA $\Delta$ 3 with glutaraldehyde. TBCB at 1  $\mu\text{M}$  and  
48 TBCBA $\Delta$ 3 at 1.5  $\mu\text{M}$  were analyzed in SDS-PAGE in the presence and absence of  
49 glutaraldehyde (at 0.05%). EB1 at 1.5  $\mu\text{M}$  was used as control (dimeric protein).  
50  
51 b) Analytical ultracentrifugation of TBCB. Sedimentation velocity experiments  
52 performed at 160,000  $\times g$  and 20°C were analyzed to yield an estimated molecular mass  
53 of 25.5 kDa, in agreement with the molecular mass of the theoretical monomer (27 kDa).  
54 See also Figure S2.  
55  
56  
57  
58  
59  
60  
61  
62  
63  
64  
65

1  
2  
3  
4 **Figure 4. YFP:TBCB is associated to the centrosome and mitotic**  
5 **microtubules**

6  
7 A) Confocal microscopy image of YFP:TBCB localization in interphase (top, left) and  
8 mitotic HeLa cells. YFP:TBCB is mostly cytoplasmic and concentrates at the  
9 centrosomes of interphase and prophase HeLa cells (top, center, arrows). In anaphase A,  
10 YFP:TBCB is clearly associated with spindle microtubules, also decorating microtubules  
11 bridging the midzone (bottom left, arrow). A midbody localization pattern is more  
12 obvious during anaphase B and telophase (bottom images, arrow), where there is no  
13 longer a centrosomal signal.

14  
15 B) Relationship of the YFP:TBCB signal with respect to the primary cilium in G1 (left)  
16 and G2 HeLa cells (right). Glutamylated tubulin labeling the primary cilium is  
17 recognized by the GT335 antibody (red).  
18  
19  
20  
21

22 **Figure 5. Microtubules bound EB1, Hsp90, and CCT are interactors of**  
23 **TBCB**

24  
25 a) Search for TBCB partners using affinity chromatography. Purified TBCB $\Delta$ 3 was  
26 purified and coupled specifically to a Hi-Trap NHS-activated HP column (GE-  
27 Healthcare). Human HEK293 protein extract (1 mL at 18 mg/ml) was applied to the  
28 column. Bound proteins were eluted using a NaCl gradient (red line). Absorbance  
29 intensity at 280 nm (Y-axis) is plotted against the collected volume (X-axis).

30  
31 b) SDS-PAGE analysis of the fractions eluted from the NHS column. Lane 1: Molecular  
32 mass marker; lane 2: aliquot of the cell extract (Control); Lane 3: FT, unbound proteins  
33 eluted in the void volume (flow-through); lanes 4–15: fractions eluted with 100–200 mM  
34 of NaCl.  
35  
36

37 **Figure 6. EB1 prevents TBCB $\Delta$ 3 microtubule destruction.**

38  
39 a) Triple-labeled confocal microscopy projection images of TBCB $\Delta$ 3 overexpression on  
40 HeLa cells. TBCB $\Delta$ 3 (green) produces conspicuous microtubule destruction (filled  
41 arrow). Moderate TBCB $\Delta$ 3 levels also severely affect the microtubule cytoskeleton  
42 (empty arrow).

43  
44 b) Statistical analysis of the proportions of cells containing normal, abnormal, or absent  
45 microtubules in TBCE, TBCB, and TBCB $\Delta$ 3 overexpressing HeLa cells 24 and 48 hours  
46 after transfection. A highly significant increase in cells containing a completely destroyed  
47 microtubular cytoskeleton is observed when the TBCB $\Delta$ 3 mutant is overexpressed  
48 compared with the wild-type construct. See also Figures S3 and S4.  
49  
50

51 **Figure 7. Models of TBCB auto-inhibition, interaction with CCT and with**  
52 **EB1 at the microtubule end**

53  
54 (a) The C-terminal region of TBCB functions as an autoinhibitory peptide when bound to  
55 the CAP-Gly domain of the protein.

56 The three domains of TBCB are depicted. The N-terminus contains the UBL (Fig 1, PDB  
57 ID, 1V6E, green). The central domain is a coiled-coil domain (CC in yellow), and the C-  
58  
59  
60  
61  
62  
63  
64  
65

1  
2  
3  
4 terminal domain contains the CAP-Gly domain (PDB ID, 1V6E, blue/purple). The acidic  
5 tail of CAP-Gly domain is shown in red and orange. We propose that the C-terminal tail  
6 of TBCB is responsible for the autoinhibition of the protein (red peptide) through the  
7 interaction with the CAP-Gly domain (blue), specifically with the highly conserved  
8 hydrophobic cavity present in the CAP-Gly domain (light blue). In contrast, if the C-  
9 terminus region does not interact with the CAP-Gly domain (orange peptide), the protein  
10 is derepressed. The hypothetical models of TBCB $\Delta$ 3 and TBCB $\Delta$ 9 showing the structure  
11 of the protein lacking the last three or nine amino acids are shown.  
12

13  
14 b) Model of TBCB-mediated  $\alpha$ -tubulin folding bound to CCT. In a first step, prefolding  
15 transfers  $\alpha$ -tubulin polypeptides (yellow) to CCT (PDB ID, 2XSM, grey) [34]. After the  
16 binary complex is formed with CCT, the  $\alpha$ -tubulin, which is in quasi-native state,  
17 interacts with TBCB that would be attached to the chaperonin to follow quickly with the  
18 postchaperonin folding pathway necessary for the incorporation of properly folded  
19 tubulin dimer ( $\alpha\beta$  tubulin) to the microtubule avoiding the transit of the monomer  
20 through the cytoplasm or degradation by the proteasome pathway [35].  
21

22  
23 c) Model of TBCB-mediated microtubule dynamics. Microtubules polymerize by  
24 addition of GTP-tubulin dimers (PDB ID, 1TUB, yellow/blue). After they are  
25 incorporated into the microtubule, the GTP bound to the  $\beta$ -tubulin subunit is hydrolyzed  
26 to GDP (yellow/light blue). EB1 (orange) is an intrinsic +TIP protein that specifically  
27 decorates growing microtubule plus ends. EB1 can bind to other +TIP proteins, such as  
28 CLIP-170 and p150<sup>Glued</sup>, through a CAP-Gly domain (PDB ID, 2HL5, pink) and may  
29 displace its theoretical C-terminal inhibitory tail. Although EBs show an elongated  
30 conformation in solution [40], TBCB does not interact with EB1 in vitro supporting an  
31 autoinhibition model similar to that proposed by Hayashi and coworkers in 2005 [38]. In  
32 any case, the elongated EB1 protein would bind specifically to the microtubule tip and  
33 not the lattice [40], and the C-terminal tail would be oriented away from the MT tip or  
34 masked by a CAP-Gly-containing protein. The motif DEI/M-COO<sup>-</sup> present in TBCB is  
35 responsible for its autoinhibition but when derepressed induces microtubule  
36 depolymerization. Once EB1 is on the microtubule, it would be recognized by TBCB  
37 inducing EB1 detachment. In addition, TBCB might be the target for TBCE, inducing  
38 tubulin dimer dissociation. As a result of these interactions, microtubules would be  
39 directed to a catastrophe.  
40  
41  
42  
43  
44  
45  
46  
47  
48  
49  
50  
51  
52  
53  
54  
55  
56  
57  
58  
59  
60  
61  
62  
63  
64  
65



Figure 1

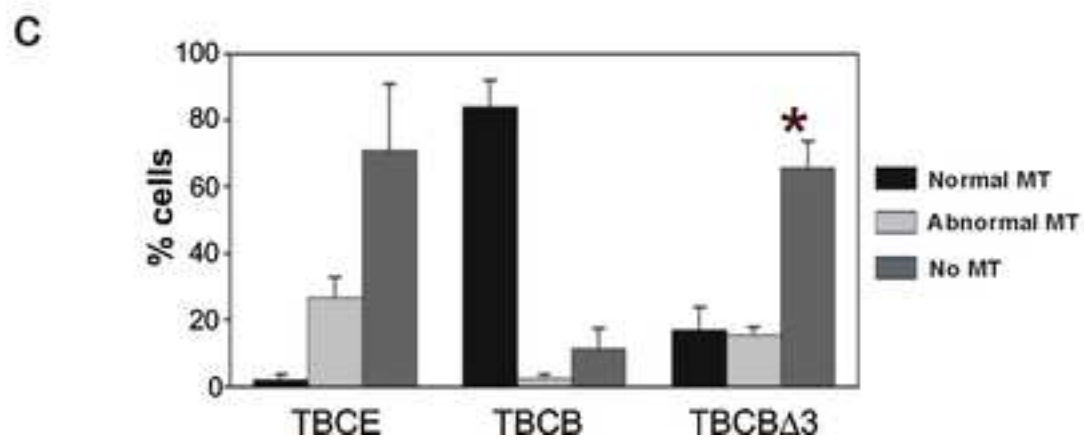
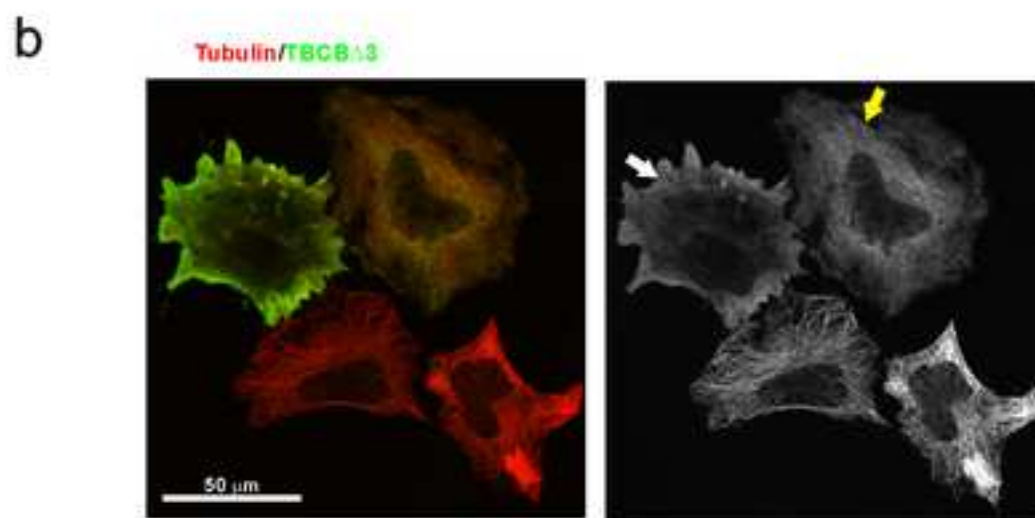
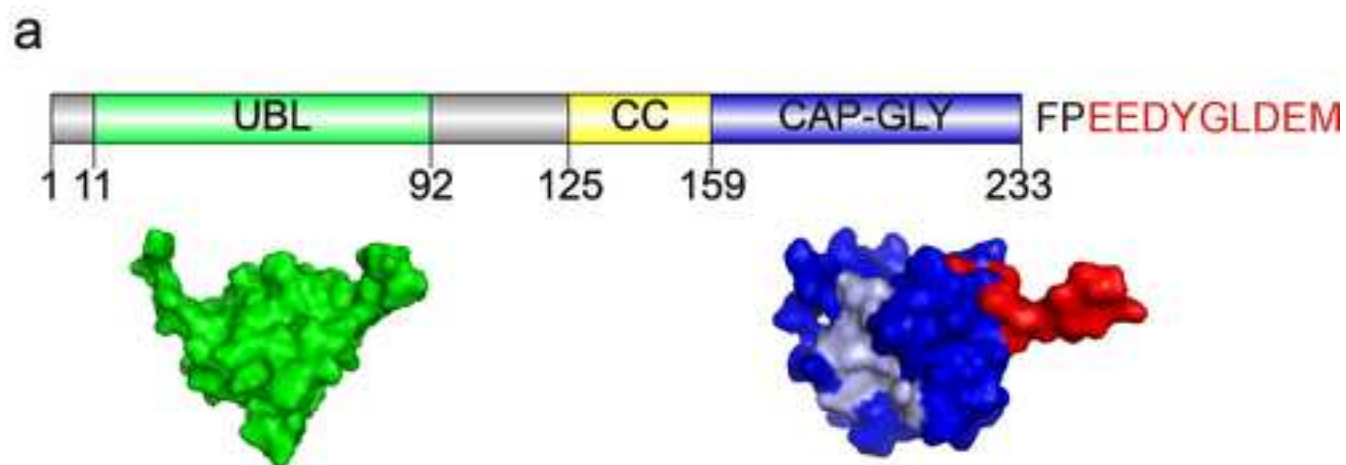


Figure 2

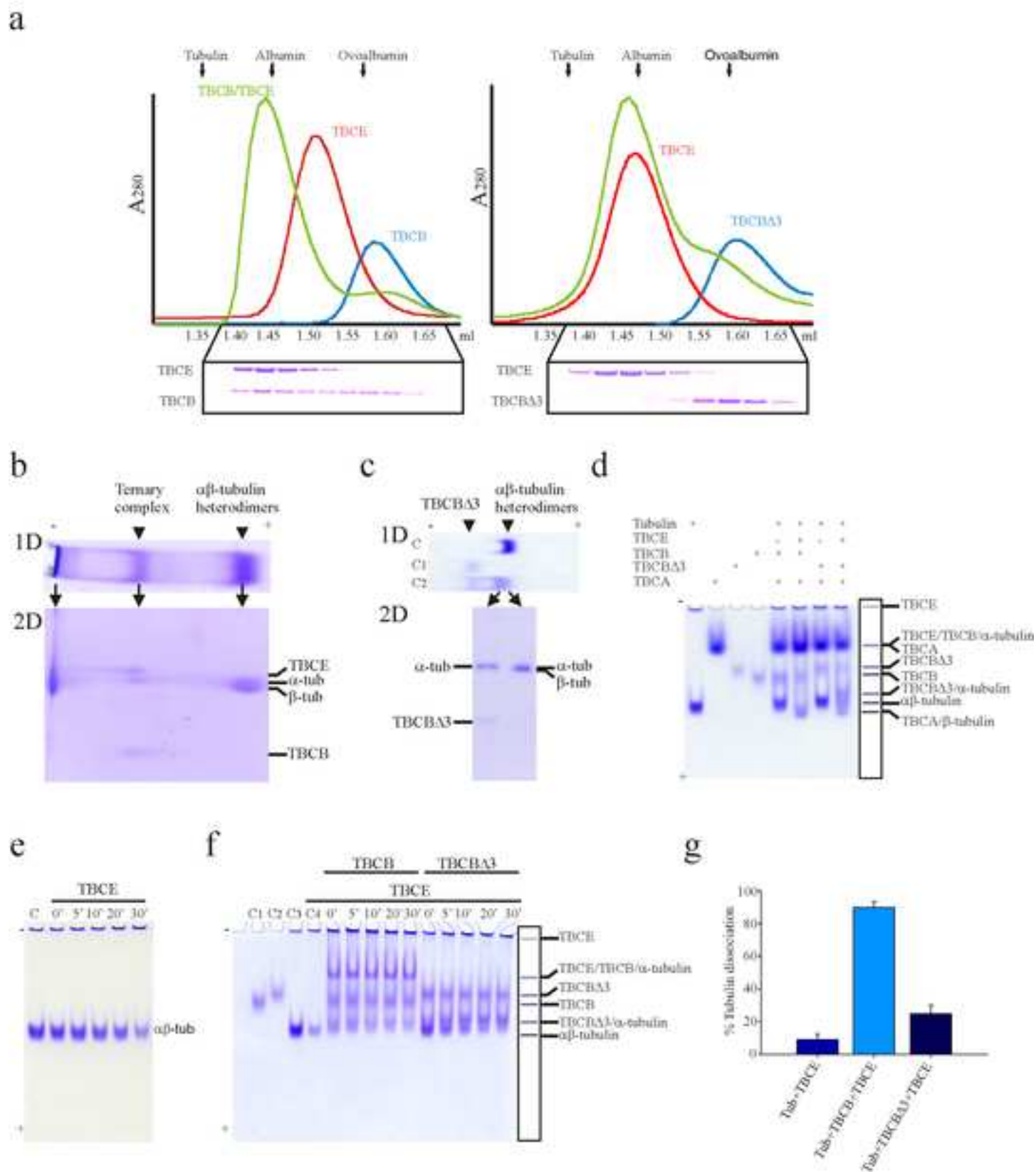
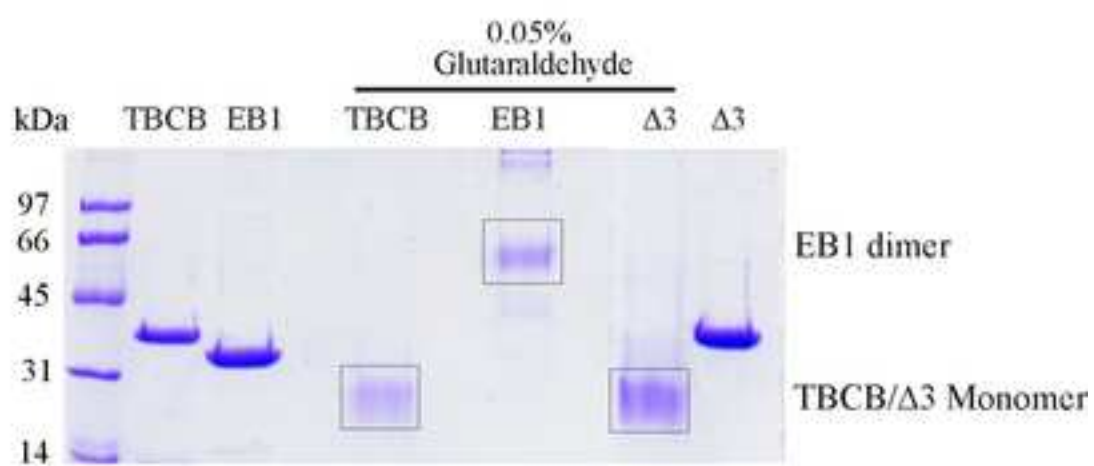


Figure 3

a



b

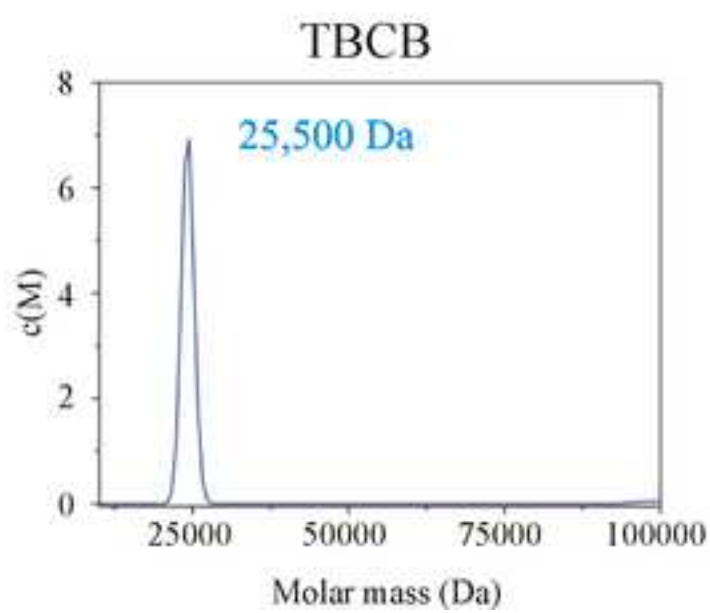
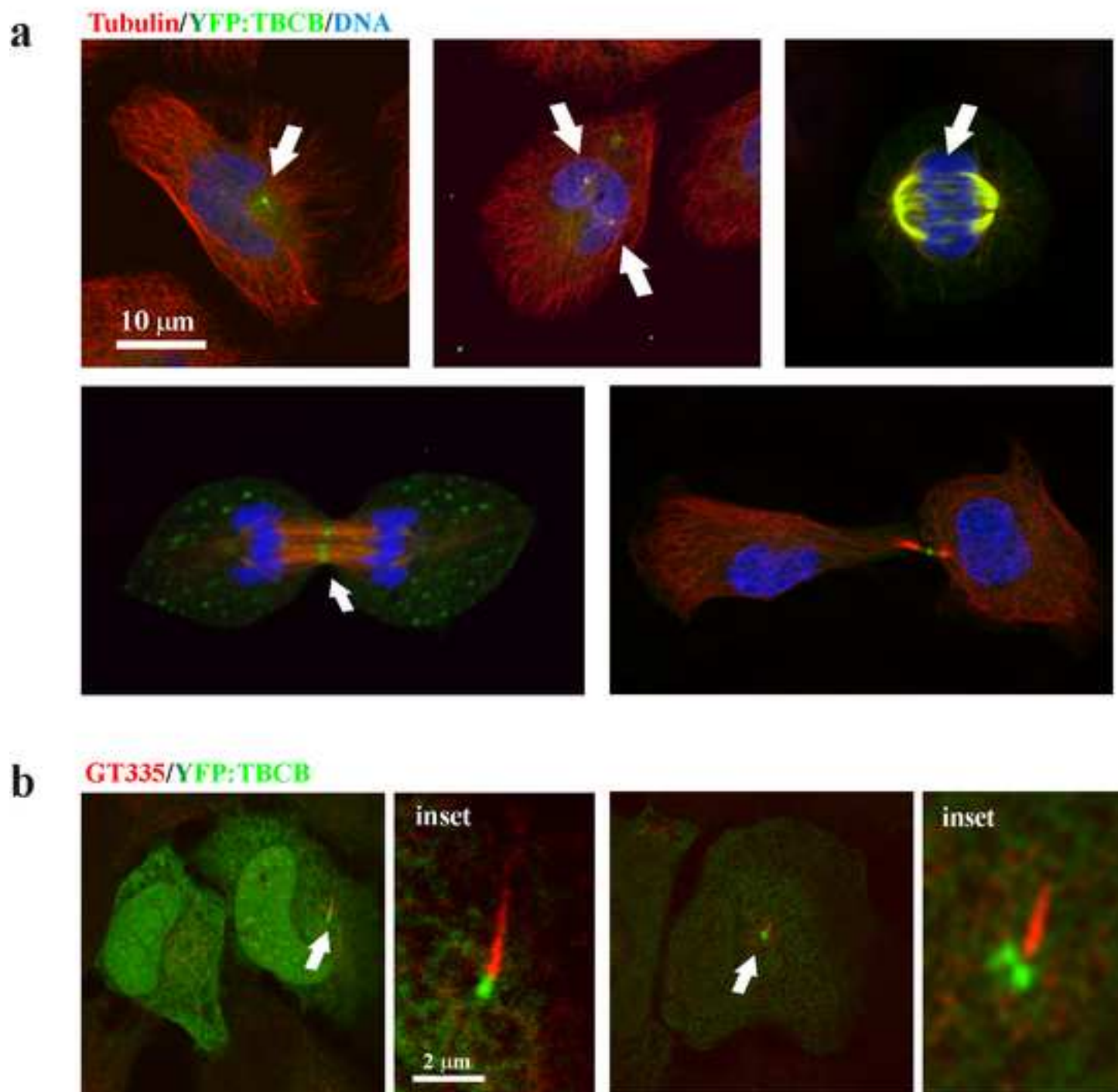


Figure 4



### Figure 5

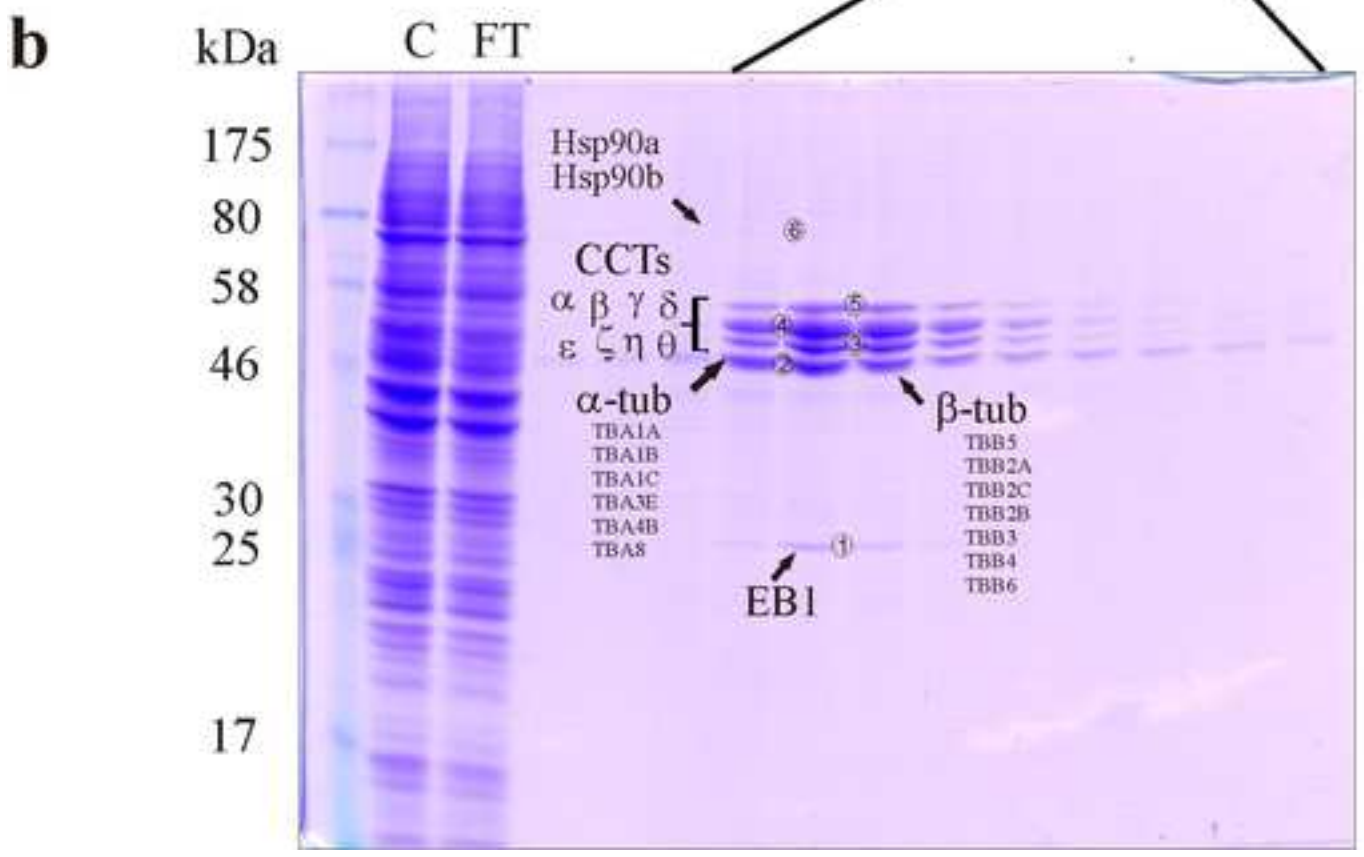
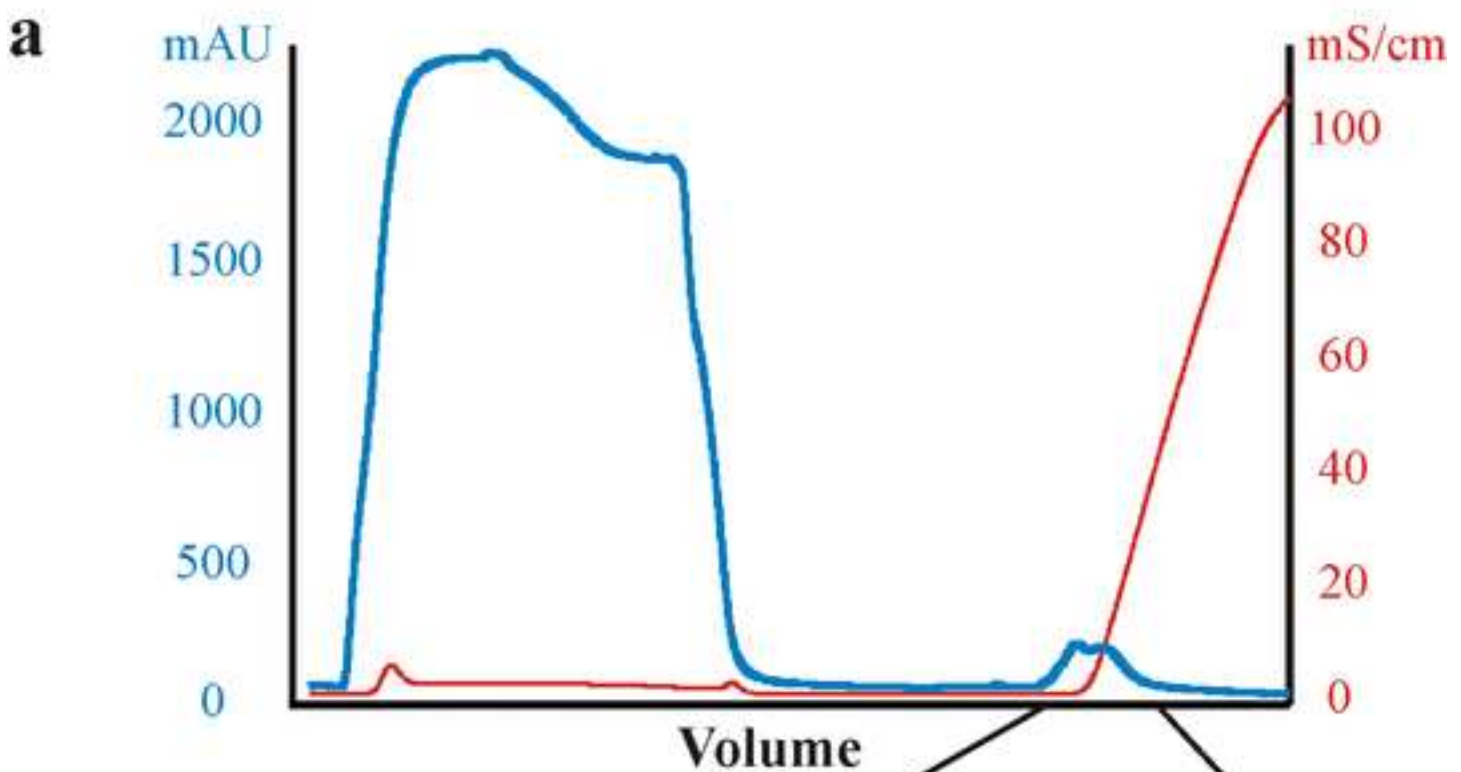
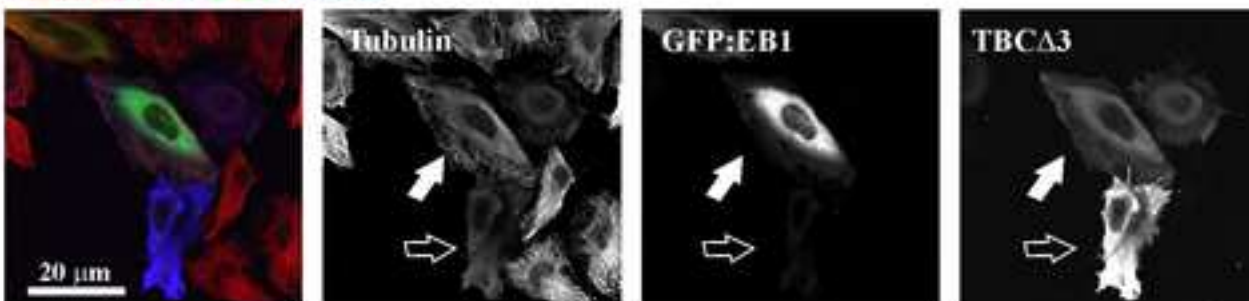


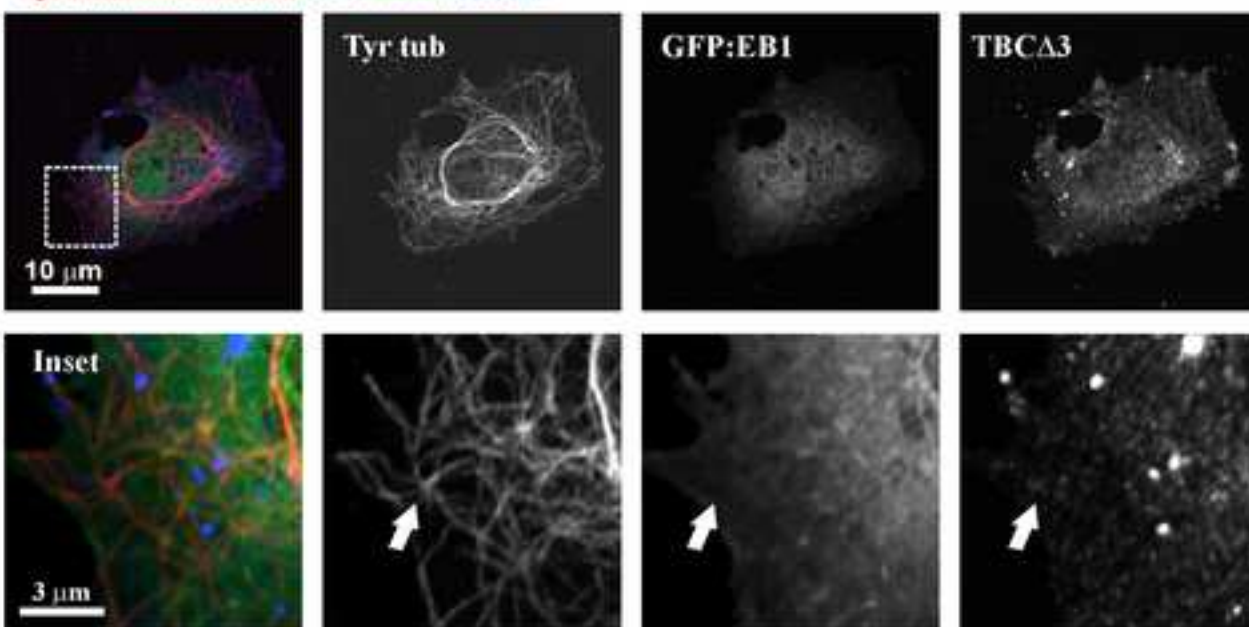
Figure 6

a

**Tubulin/GFP:EB1/TBCA3**



**Tyrosinated tubulin/GFP:EB1/TBCA3**



b

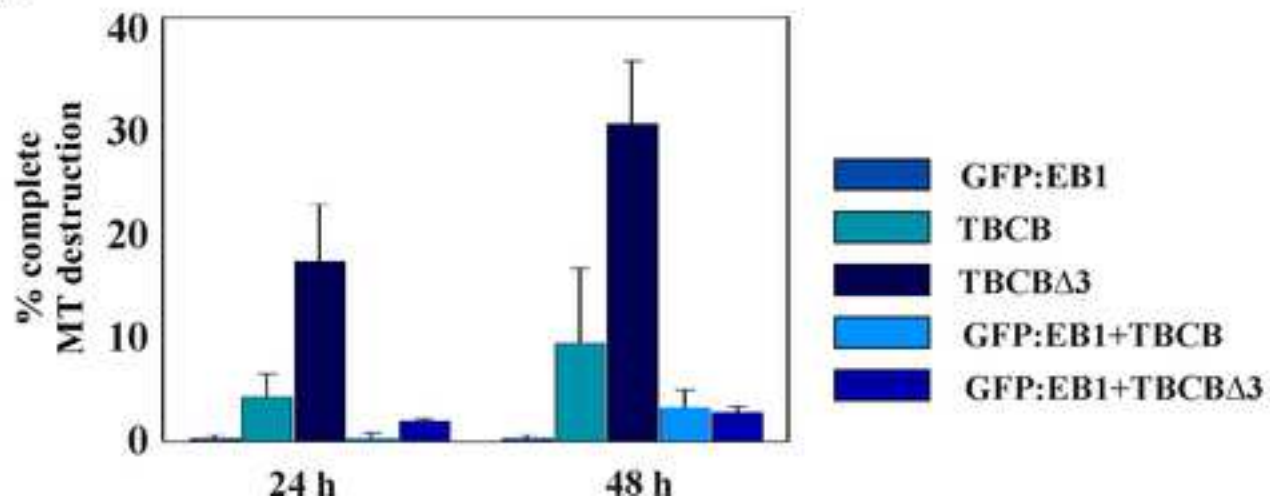
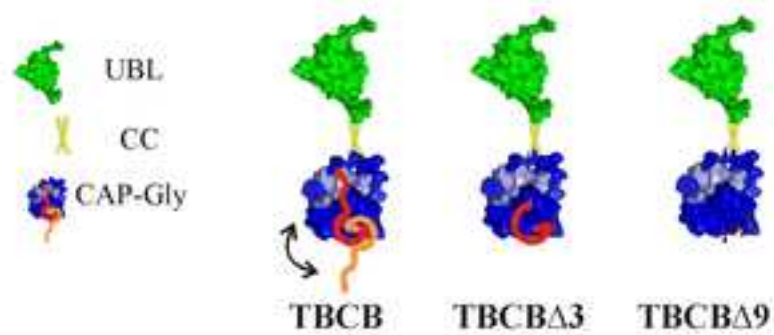
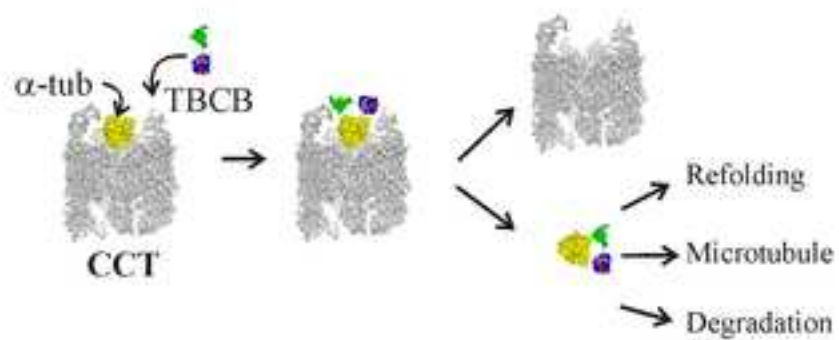


Figure 7

a



b



c

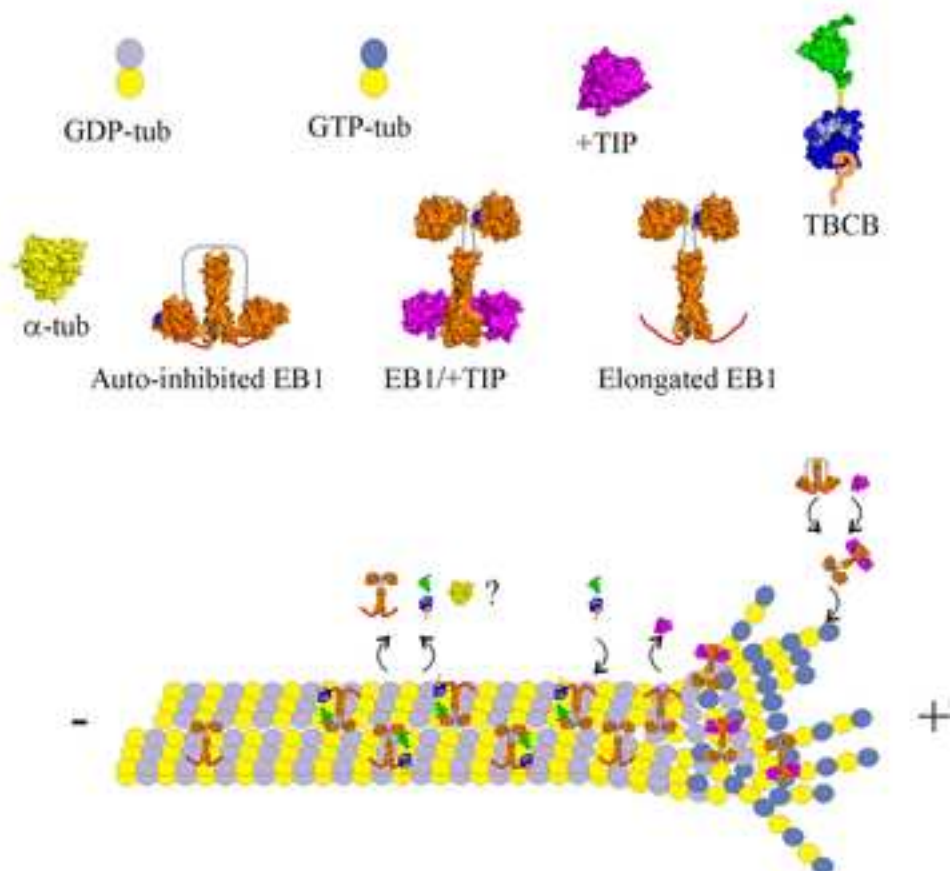


**Table 1.** Determination of the equilibrium dissociation constants for the binding of the fluorescein labeled TBCB and  $\alpha$ -tubulin peptides to TBCB, TBCB $\Delta$ 3, and TBCB $\Delta$ 9 by fluorescence polarization (FP). FP binding assays of TBCB with FL-peptides were repeated up to a protein concentration of 100  $\mu$ M (FigS5). See also Figure S5.

Peptide	Protein	Kd, $\mu$ M
EEDYGLDEI (TBCB)	TBCB	12 $\pm$ 1
"	TBCB $\Delta$ 3	74 $\pm$ 3
"	TBCB $\Delta$ 9	79 $\pm$ 4
EEDYGL (TBCB $\Delta$ 3)	TBCB	71 $\pm$ 3
"	TBCB $\Delta$ 3	178 $\pm$ 15
"	TBCB $\Delta$ 9	249 $\pm$ 30
GEGEEEGEEY( $\alpha$ 1/2-tub)	TBCB	43 $\pm$ 2
"	TBCB $\Delta$ 3	113 $\pm$ 7
"	TBCB $\Delta$ 9	145 $\pm$ 9
GEGEEEGEE( $\alpha$ 1/2-tub $\Delta$ Y)	TBCB	140 $\pm$ 4
"	TBCB $\Delta$ 3	312 $\pm$ 20
"	TBCB $\Delta$ 9	472 $\pm$ 69



Supplementary Material

[Click here to download Supplementary Material: Supplemental Carranza.pdf](#)